# Variable Air Volume Hot Water Reheat Terminal Units

## Temperature Stratification, Performance at Low Hot Water Supply Temperature, and Myths from the Field

**Patrick Wendler, EIT**
Graduate Student Researcher, Center for the Built Environment, UC Berkeley

Paul Raftery, PhD
Researcher, Center for the Built Environment, UC Berkeley

Hwakong Cheng, PE
Principal, Taylor Engineers


**January 2023**

# ACKNOWLEDGEMENTS

The California Energy Commission project (grant: PIER-19-013) and the Center for the Built Environment provided funding for this work. We would like to thank Dale Paskaruk, Alberto Bathan, Mark Mahon, Mike Koupriyanov, and Graham Fediuk of Price Industries for facilitating the testing, Steve Taylor for technical advice, and the broader project team who reviewed and gave suggestions to improve the paper.

Note that some of the contents of this paper were previously published as a conference paper for the ASHRAE 2023 Winter Conference in Atlanta, GA (Wendler et al., 2023). The paper will be the subject of a presentation to be delivered at the conference on February 5, 2023. The contents of this ASHRAE conference paper reflect more limited findings of the experiment described herein. As such, the current paper reflects the most complete findings and the most up-to-date results and recommendations.

**CREDIT STATEMENT:**

**Patrick Wendler:** Experiment design, Performance of testing, Data curation, Methodology, Visualization, Writing – original draft. **Paul Raftery:** Conceptualization, Data curation, Funding acquisition, Investigation, Methodology, Project administration, Resources, Supervision, Visualization, Writing – review & editing. **Hwakong Cheng:** Methodology, Resources, Data curation, Investigation, Writing – review & editing.

# ABSTRACT

Hot water coils are common in commercial building HVAC systems. Nevertheless, their design, installation, and control are frequently sub-optimal, with respect to maximizing heat exchange effectiveness and air temperature setpoint control. For example, conditions on-site sometimes lead to coils being installed in parallel flow instead of counter flow configuration, and temperature stratification in the leaving air can lead to control issues. Additionally, low hot water supply temperatures (HWST) of ~120ºF (49ºC) are becoming more common with the rise of heat pump and efficiency retrofits. As hot water systems are typically designed for high HWST (160 - 180ºF, 71 - 82ºC), lower waterside "delta T" temperature differences (HWST – HWRT) would occur using low HWST in retrofits of conventional hot water heating systems. If buildings retain existing coils for the low-HWST systems common to efficiency retrofits, they will be unable to maintain the same design heat capacity without replacing terminal units. This creates challenges for retrofit projects throughout the industry, and low-HWST designs also present challenges to new construction. We present the background, methods, and findings of an experiment conducted in 2022 at the Price Industries Laboratory in Winnipeg, Canada. In this experiment, we tested multiple VAV HW reheat terminal units across a range of test factors, including VAV box sizes and number of coil rows. The performance of each coil setup was compared at both high and low HWSTs, and at multiple damper positions. We also performed several additional tests to determine the best solutions to common field installation and operation issues and to gauge the impact of varying coil insulation. In addition to tests we ran with stock-manufactured coils, we also ran several tests using coils of our own custom designs, focusing on symmetry and limited circuit count. The intent of these tests was to better understand the factors in VAV HW reheat systems that may be overlooked in typical system design and coil selection processes, especially as parameters such as HWST and water side temperature differences begin to change. Understanding these factors is important to the design and operation of these systems as sub-optimal performance in the terminal unit systems has cascading effects both for retro-fitted low-HWST systems and existing boiler systems. Overall, the results from this experiment serve to inform recommended changes to VAV terminal unit design, selection, and control to improve whole-building performance.

**Keywords**: VAV, reheat, coils, hot water, temperature stratification, low HWST, damper position, coil circuiting, sensors, controls

# TABLE OF CONTENTS

# LIST OF FIGURES

# EXECUTIVE SUMMARY

This paper presents the background, methods, and results of an experiment we conducted in 2022 to test the performance of variable air volume (VAV) hot water reheat systems under various conditions. Based on our results, we present several recommendations to change industry standards, equipment design, and common installation and operation practices associated with VAV reheat systems.

## Background

Multiple factors impacting the performance of conventional VAV HW reheat systems are often overlooked in standard rating methods and design practices. These include losses in the distribution system, temperature stratification downstream of the reheat coil, and the impact of damper position on coil capacity.

Industry-standard testing methods used to select coil types and sizes do not consider factors such as the presence of dampers and provide no guidance for the optimal mounting location of the controlling discharge air temperature sensor in the plenum. This limits modeling accuracy and information available to designers selecting coils and designing controls for systems with high airflow and static pressure variability. In buildings undergoing retrofits that seek to lower the HWST (as is common in many electrification retrofits), waterside temperature differences will decrease if existing heating system components are left in place, and coil heating capacity decreases substantially. To maintain design heating capacity, designers need to choose between increasing the size of the system components (which would be prohibitively expensive), or selecting and installing coils selected for low HWST (which is rarely feasible from a first cost perspective and for which standard modeling methods overlook various real-world performance factors), or adding supplemental heating capacity, or reducing heating loads. Without somehow addressing this issue, electrification and major efficiency retrofit projects are often infeasible.

## Experiment and Objectives

The experiment we conducted aimed to explore the performance of coils operating under real-world conditions that standard rating methods and design practices do not currently account for. To do this, we tested multiple VAV HW reheat terminal units across a range of test factors, such as box size and number of coil rows, damper positions, and HWST. The objectives are to:

1. Determine the impact of damper position.
2. Determine the extent and impact of discharge air temperature stratification.
3. Determine the level of heat loss that occurs through uninsulated components.
4. Recommend improved selection methods and controls.
5. Highlight solutions to common field installation challenges.

We conducted the experiment using a mock-up VAV reheat system with several different coil types and box sizes. We also varied the hot water supply temperature (HWST) and damper position as we took the measurements needed to support the experiment goals.

# Results and Recommendations

Our results and associated recommendations are as follows:

## Results

1. Coil heating capacity decreases as the damper closes (while air and water flow are held constant).
2. Discharge air temperature and air velocity are considerably stratified within the outlet duct. This effect tends to worsen as the damper closes.
3. With the valve train, associated supply and return piping, and coil housing uninsulated, heat losses can be as large as 750 BTU/hr (220 W), which is equivalent to losses resulting from 15 ft (4.6 m) of uninsulated ¾" pipe at 160ºF (71ºC).
4. When installing a left-handed coil in a right-handed orientation, connecting the HWS piping at the bottom of the coil (parallel flow) can result in capacity losses up to 10% relative to installing the HWS piping at the top of the coil (counter flow).
5. In zone control systems that keep hot water flowing through coils while their respective zones are unoccupied and airflow is shut off, heat losses of 2.1 kBTU/hr (0.61 kW) at 160ºF HWST and 1.3 kBTU/hr (0.38 kW) at 120ºF HWST are possible. This represents about 7% of design capacity in both cases.
6. Using coils with custom-designed circuiting, we observed capacity to increase in these coils relative to their stock design counterparts

## Recommendations

1. Designers should ensure static pressure reset sequences are implemented and operating well in VAV reheat systems to minimize heating capacity losses at more closed damper positions.
2. Designers should mount single-point DAT sensors as close to the centerline of the duct as possible, as far from the coil as possible.
3. Designers and builders in new construction projects should insulate all valves, pipes, coil components and housing, while in retrofits, these should be insulated at the same time as other VAV box measures.
4. Any applicable guidance (e.g. from manufacturer documents, energy codes, etc.) should incorporate the requirement for installers to maintain counter flow in all coil installations. Distributors should also stock both left- and right-handed coils to provide the proper coil for any field condition.
5. For all buildings using zone-based occupancy controls, designers should ensure that both airside and waterside controls are employed to avoid energy losses during unoccupied hours.
6. Coil manufacturers should allocate additional resources to re-designing typical coil circuiting for increased performance and ease of installation.
7. Designers can rely on coil selection software to estimate capacities at low design water temperatures more commonly encountered when designing for all-electric HVAC systems (i.e., generating heating hot water using a heat pump)

# CHAPTER 1: Introduction

## Background

Multiple factors impacting the performance of conventional VAV HW reheat systems are often overlooked in standard rating methods and design practices. These include losses in the distribution system, temperature stratification downstream of the reheat coil, and the impact of damper position on coil capacity. One case study found that just 21% of input gas energy in a large commercial building was converted into useful reheat energy, with distribution losses alone accounting for 44% of boiler heat output. Multiple case studies in similar buildings have also found that VAV systems typically operate at low-load conditions (Arens et al., 2015; Raftery et al., 2018). These low-load conditions cause distribution losses to represent a higher proportion of energy losses than would otherwise be the case in high-load conditions.

Industry-standard testing methods such as ASHRAE Standard 33 and AHRI 410 are used to select coil types and sizes for rated full-load conditions. However, these standards do not consider factors such as the impact of partially-closed damper positions, which is the most common operating condition for heating coils in VAV terminal units. The standards do not specify the use of dampers in the test at all, as they aim to test fully uniform flow across the coil. Similarly, no standard design guidance exists for the optimal mounting location of the controlling discharge air temperature sensor in the plenum. This limits modeling accuracy and information available to designers selecting coils and designing controls for systems with high airflow and static pressure variability. In buildings undergoing retrofits that seek to lower the HWST from 160-180ºF (71 – 82ºC) to 120ºF (49ºC), waterside temperature differences will decrease if existing piping, coils, and pumps are left in place, and coil heating capacity decreases substantially. To maintain design heating capacity, designers need to choose between increasing the size of the pumps and piping (which would be prohibitively expensive even if it is feasible to meet the required capacity needs), or selecting and installing coils selected for low HWST (which is rarely feasible from a first cost perspective outside of gut renovations, and for which standard modeling methods overlook various real-world performance factors), or adding supplemental heating capacity, or reducing heating loads. Without somehow addressing this issue, electrification and major efficiency retrofit projects are often infeasible.

## Objectives

The experiment we conducted aimed to explore the performance of coils operating under real-world conditions that standard rating methods and design practices do not currently account for. To do this, we tested multiple VAV HW reheat terminal units across a range of test factors, such as box size and number of coil rows, damper positions, and HWST. The objectives are to:

1. **Determine the impact of damper position** on heating capacity in typical operating conditions.
2. **Determine the extent and impact of temperature stratification** downstream of the reheat coil.

3. **Determine the level of heat loss that occurs through uninsulated components** such as the coil frame, manifolds, tube bends, and valve train relative to fully insulated components.
4. **Recommend improved selection methods and controls** that account for real-world conditions.
5. **Highlight solutions to common field installation challenges** that optimize coil performance.

# CHAPTER 2: Method

## Testing Apparatus and Lab Facilities

The test apparatus consisted of an inlet duct, typical VAV box, hot water coil, and outlet plenum equipped with sensors and air mixers. The apparatus was contained within a psychrometric chamber with connections to variable flow supply and return fans. The majority of tests were run with a "blow-through" configuration, in which the inlet duct was connected to the discharge of the supply fan, which blew air through the duct and coil assembly into the ambient air of the chamber. Design heating airflow for each box size, as dictated by Guideline 36, was maintained based on flow cross readings at the box inlet. The inlet air temperature was maintained at 57ºF (14ºC) based on RTD readings at the box inlet. A minority of tests were run with "draw-through" arrangement, in which the intake of the supply fan was connected to the plenum discharge and the inlet duct was open to ambient air maintained at a constant 57ºF (14ºC). Design airflows in this configuration were maintained based on readings from a nozzle bank downstream of the plenum discharge. In both configurations, one to three 25-point thermocouple arrays were installed in the discharge plenum to measure discharge air temperature stratification. We found negligible differences for coil capacity and discharge air temperature results between the "blow-through" and "draw-through" configurations. The "blow-through" configuration was selected as the dominant method as it directly reflects real-world operating conditions, and due to the positive pressure difference, ensures that any leakage will be to the room from the box, instead of vice versa (which could potentially affect temperature stratification readings).

A variable speed pump supplied hot water to the coil. The water supply was routed through one of two flowmeters located outside the psychrometric chamber, with one flow meter reserved for high flow conditions (6-60 gpm, 23-230 Lpm) and the other reserved for low flow conditions (1 - 12 gpm 4-45 Lpm). The lengths and sizes of the ducts, as well as the operating parameters used in each were determined based on published best practices (Steve Taylor, 2015; Steve Taylor & Jeff Stein, 2004). Unlike the differing airside configurations, neither the fluid side configurations nor the duct size selection methods were changed throughout the experiment. **Error! Reference source not found.** shows a diagram and photo of the testing apparatus in the "blow-through" configuration.

**Figure 1: Testing Apparatus**

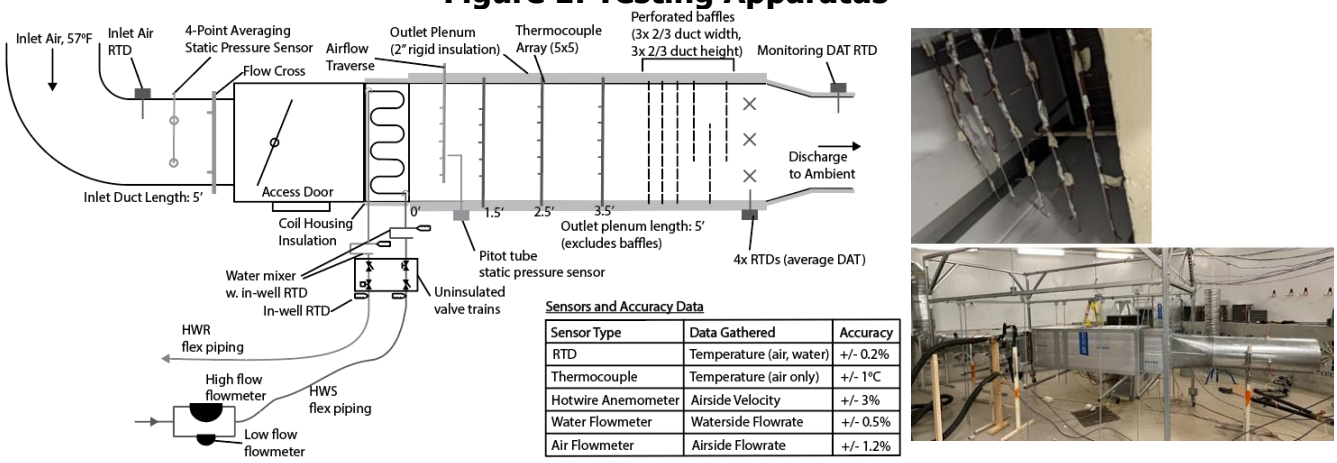


Sensors and Accuracy Data

| Sensor Type | Data Gathered | Accuracy |
|---|---|---|
| RTD | Temperature (air, water) | +/- 0.2% |
| Thermocouple | Temperature (air only) | +/- 1ºC |
| Hotwire Anemometer | Airside Velocity | +/- 3% |
| Water Flowmeter | Waterside Flowrate | +/- 0.5% |
| Air Flowmeter | Airside Flowrate | +/- 1.2% |





**Testing apparatus diagram (left), thermocouple grid (top right), testing apparatus photo (bottom right)**

## Sensors and Data Acquisition

We mounted three 5x5 thermocouple grids at even spacing down the length of the outlet plenum to measure temperature stratification in the airstream. To measure air speed stratification, we took velocity traverses at a point fifteen inches (15") downstream of the coil using a hotwire anemometer. We selected measurement points in each air speed traverse and thermocouple grid using the log-Tchebycheff method for duct traverses, as indicated in ASHRAE Standard 41.2. We used ten RTD temperature sensors throughout the test apparatus. One RTD was inserted into a forced air psychrometer to measure the ambient air entering the inlet duct. Four RTDs were mounted at the end of the outlet plenum and averaged together to measure the discharge air temperature (DAT). This averaged DAT was used to calculate airside coil capacity. One RTD was mounted further downstream of the four averaging RTDs to monitor DAT and provide a value against which to check the average DAT used in calculations. The final four RTDs were in-well sensors that measured waterside temperatures. We used the water flow meters and air flow meter, along with the respective temperature differences, to calculate the waterside and airside heat transfer. Throughout the paper we report waterside capacity, unless otherwise noted.

# Testing Procedure

We followed the ASHRAE Standard 33 test procedure with one primary difference: we tested the coil in an actual VAV box, including the damper and related flow disturbance, rather than the much more uniform flow conditions required by the test standard. For our procedure, we ran each test by allowing the system to reach steady state, then averaged data collected over fifteen (15) minutes in 1-minute intervals.

# Variable Testing Factors

We ran each test with a unique combination of box size, number of coil rows, and HWST. We ran 108 tests in total with the following factors: HWST (120 ºF n=62, 160 ºF n=46), box size (12" n=59, 8" n=31, 12" oversize n=9, 8" oversize n=9), coil rows (1-row n=29, 2-row n=52, 3-row n=27). We chose operating factors such as air and water flow based on the HWST, box size, and coil rows to maintain a leaving air temperature of 90ºF (32ºC).

For a select few tests, we varied other factors to isolate the impact of certain conditions: coil and valve train insulation (fully insulated vs. uninsulated), damper rotation (clockwise vs. counter-clockwise), and piping orientation for an inverted left-hand coil (HWS connected at the top vs. bottom of the coil). We also ran two tests with airflow turned off to measure heat loss from the coil when the valves are open even if the air handlers are off (which sometimes occurs in practice). Note that for each category above, the factors were not tested in every possible combination (i.e. the tests were not a full factorial) as some combinations would yield unrealistic selections for typical VAV box applications (e.g. single-row coils in oversize boxes, 3-row coils with high HWST).

# CHAPTER 3: Results & Discussion

## Impact of Damper Position

For each coil and box size pairing, we ran tests with 120 ºF (49ºC) and 160 ºF (71ºC) HWST (except for tests with 3-row coils, which only ran at 120 ºF). At each level of HWST, we modulated the damper position at three (3) to four (4) levels from 100% open to 27% open, with airflow held constant for each box and coil combination as measured by either the flow cross (as in a real system) or a more accurate nozzle bank measurement. The only varying factor was static pressure (and damper position) while airflow, water flow, and supply temperatures remained constant, reflecting real-world operation of pressure independent VAVs. We collected waterside heat transfer data at each damper position to examine the change in coil capacity and to compare the measured capacities against the rated capacities obtained from AHRI 410 certified manufacturer's modelling software (**Error! Reference source not found.**a). The propagated instrument uncertainty in the measured capacities was median 1.1% (0.9% Q1, 2.0% Q3), while the median percent difference of the measured capacities vs. those obtained from the AHRI 410 certified modelling software was -1.9% (-8.3% Q1, 1.1% Q3) (Figure 2b).

**Figure 2: Damper Position Capacity Effects**

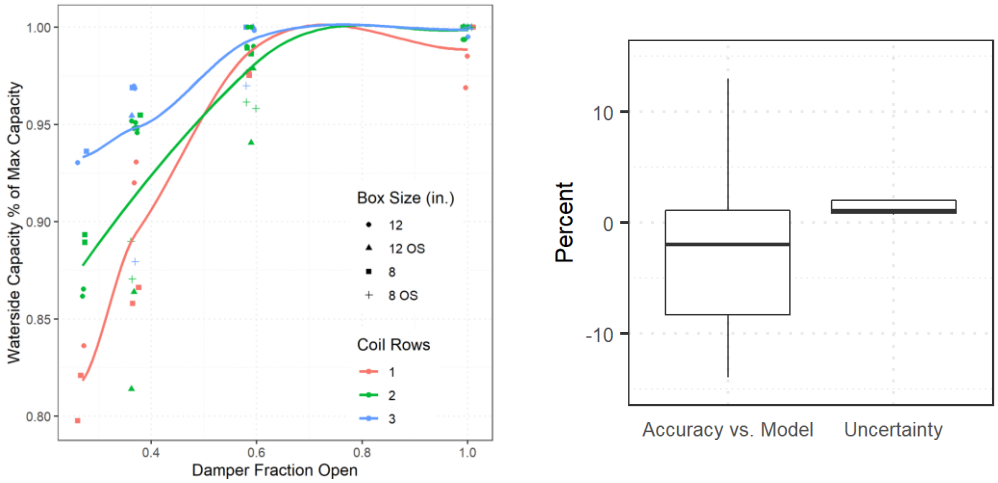


**Impact of damper on coil capacity (Figure 2a, left); Capacity measurement uncertainty and accuracy vs. capacity obtained via AHRI 410 (Figure 2b, right)**

Considering that airflow was held constant as the damper closed for each test, these results show that capacity reliably decreases as the damper closes due to the flow disturbance it causes. Across all tests, the median loss of capacity at the 37% damper position was 5.4% (4.7% Q1, 12.5% Q3), at 27% it was 13.4% (10.7% Q1, 16.4% Q3). This effect highlights for the first time the suboptimal performance of VAV boxes with coils at high static pressures, as the coil could provide up to 20% less heat than it was potentially designed for (e.g. boxes close to the air handler with high static pressure). For VAV reheat systems, this requires buildings to use higher airside and waterside flow rates than necessary to meet setpoints, or risk having insufficient capacity to meet setpoint. Many zones operate with partially closed damper positions during heating in practice, in part due to their location in the ductwork relative to air handler, but also due to unnecessarily high duct static pressure being

maintained due to the lack of a functioning duct static pressure reset logic. We recommend including duct static pressure reset sequences according to ASHRAE Guideline 36, including a very low lower setpoint limit (e.g. 0.1 in. wc). This will reduce the leakage, fan energy consumption and the negative effect of damper position on coil capacity, at least as much as possible without making physical modifications (e.g., installing balancing dampers).

## Temperature and Velocity Stratification

We measured temperature stratification in the plenum with three 5x5 thermocouple arrays placed throughout the length of the plenum in each test. We also measured velocity stratification by taking a 5x5-point velocity traverse near the most upstream thermocouple grid at each damper position and airflow pairing.

3 shows three heatmaps representing the difference between each thermocouple's measured temperature and the average temperature at each thermocouple's respective measurement plane for one representative test (12" box, 2-row coil, 160ºF HWST, 37% open damper).

**Figure 3: Temperature Stratification Heatmap**

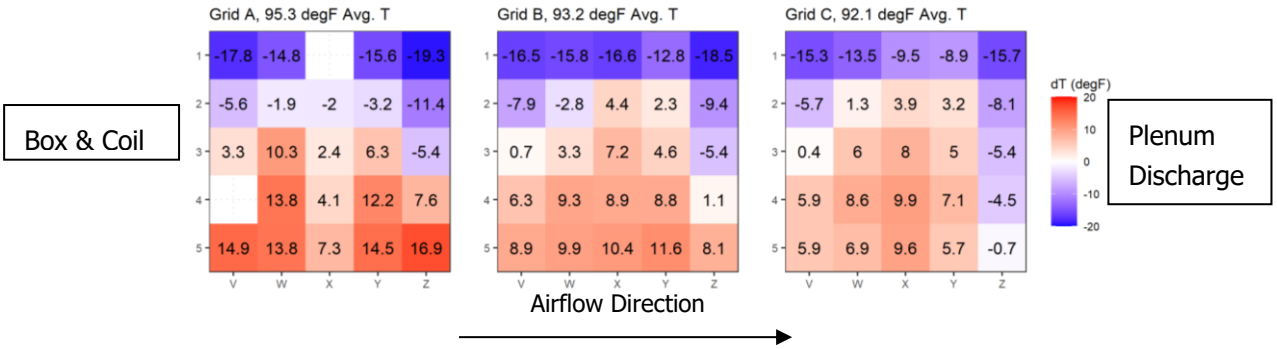


**Temperature stratifications for example test (Grid A most upstream, Grid C most downstream) – note two points have been removed from Grid A due to faulty data acquisition for the associated sensors.**

Based on these heatmaps, we can see that the coolest temperatures tend to occur at the top edge of the plenum while the warmest temperatures occur at the bottom. This effect is further illustrated by an examination of the difference in average temperatures between the side edges of the duct (columns) compared to the difference between the top and bottom edges (rows). For the majority of tests, the difference in temperatures between the top and bottom of the duct were higher than those for the sides of the duct (see Figure 4a). Temperatures closest to the average tend to occur in the nine (9) center points of the duct. The low temperatures occurring at the top of the duct can be attributed to a combination of the water in the coil being at its coldest in this area (due to it being in line with the coil return) and the higher velocity air passing over this part of the coil (due to the damper position) potentially partly bypassing the fins and flowing through a gap between the fins and the coil frame caused by the weight of the coil. The airside factors contributing to discharge air temperature stratification are therefore suspected to be a dual effect of the higher air velocities occurring at more closed damper positions as well as the gap between the coil frame and fins caused by the weight of the coil. More tests will need to be run targeting the coil frame gap to determine the severity of its impact on temperature stratification.

For each of the four damper positions, we calculated the absolute value of the difference between the measured temperature at each point and the average temperature for each point's grid. We then plotted these differences in box plots, separating by damper position and HWST. Figure 4b and 4c shows the distributions of these differences for all thermocouple points as well as the center nine (9) points.

**Figure 4: Temperature Stratification Box Plots**

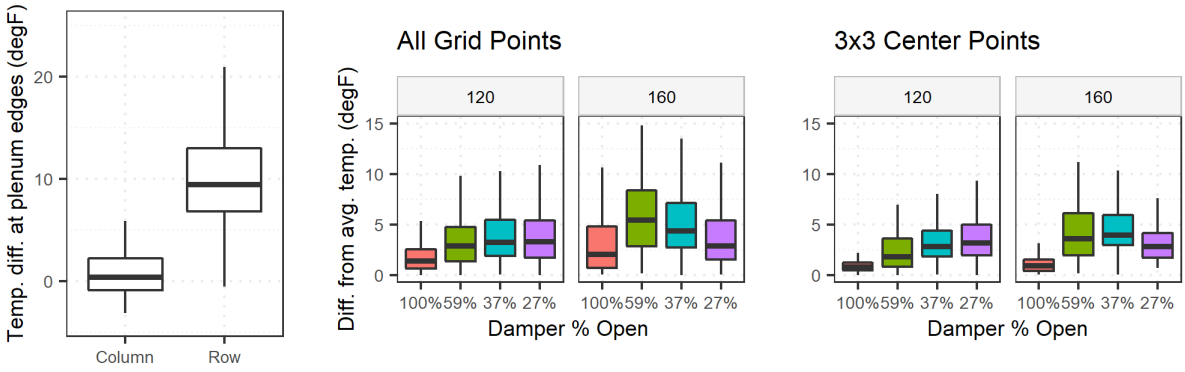


**Temperature difference between top and bottom row vs. left and right column (Figure 4a, left); Temperature stratification by damper position and HWST for all tests and all grid points (Figure 4b, center); and for nine centermost points in the duct (Figure 4c, left)**

We can see from Figure 4b and c that damper position has a substantial impact on temperature stratification, with the 27% open damper position resulting in substantially more stratification than more open damper settings, especially at low HWST. We also performed velocity traverses for 41 tests and a similar distribution occurred in velocity stratification measurements. The least amount of stratification occurs at the 100% damper position and with higher velocities occurring increasingly toward the top of the plenum as the damper closed, as expected. The average percentage of deviation from the average velocity across all tests rose from 19% for the 100% damper position up to 39% for the 27% damper position. Considering this degree of stratification together with the damper-dependent capacity losses shown in the results above, we show that as the damper closes, both temperature and velocity stratification increases, and coil capacity decreases, linking these two issues together.

One solution to address the issue of temperature stratification and the resulting variability in temperature readings is to install an averaging temperature sensor[1] in place of a conventional single-point sensor. Figure 5a and 5b show the absolute differences from the average temperature likely to be measured by a single-point sensor installed near the center of the plenum vs. a 12" averaging sensor installed along the horizontal centerline of the plenum.

[1] there are products which average 4 thermistors on a rigid straight probe of length appropriate for a VAV box application.

**Figure 5: Expected Sensor Readings**

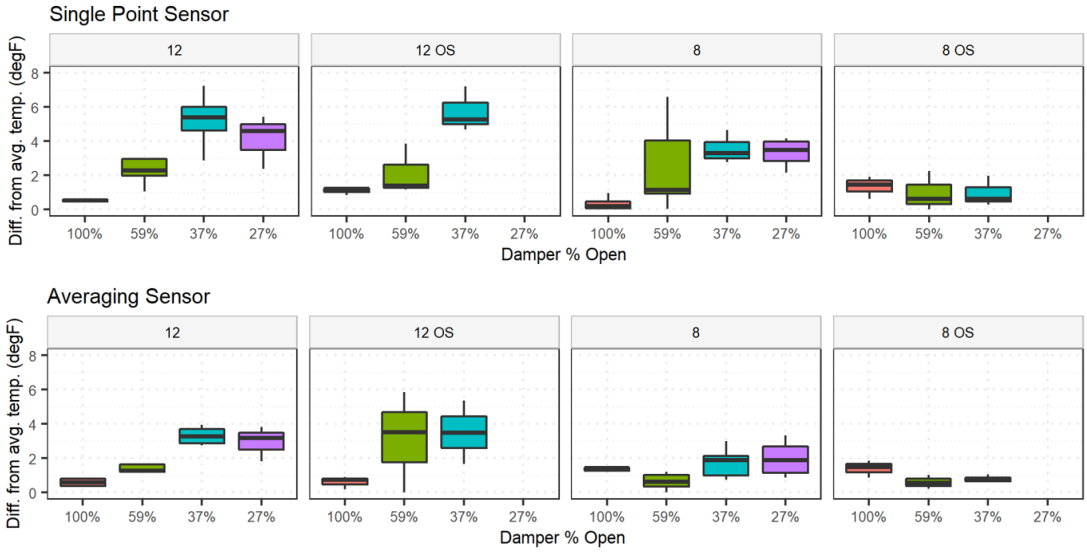


**Temperature difference from duct average for single-point sensor (Figure 5a, top) and averaging sensor (Figure 5b, bottom) (both figures grouped by box size)**

We can see from Figure 5a and b that for the vast majority of box sizes and damper positions, an averaging sensor installed along the horizontal centerline of the plenum provides readings consistently closer to the average temperature than a single-point sensor located at the center of the plenum.

Based on these findings, we can see that the readings of a discharge temperature sensor in the plenum are subject to substantial variation based on its mounting location and the modulations of the damper. While an averaging temperature sensor would best address this issue, it may be cost-prohibitive on more budget-constrained retrofit projects. If using a single-point discharge air temperature sensor, we recommend placing it as close to the centerline of the duct as possible, as far from the coil as possible. Additionally, since stratification was typically worst at the top and bottom of the duct, we recommend designers and installers to use duct taps at the sides of the plenum instead of at the top and bottom wherever possible, as the latter will yield a larger difference in air temperatures delivered to each tap.

## Impact of Damper Orientation

Dampers in VAV reheat systems mostly often open from the top (i.e. the top of the damper moves in the direction of the airflow as it opens, towards the return water outlet of the coil). To isolate the impact of the damper orientation on DAT stratification and coil capacity, we ran tests at the four damper positions with the VAV box inverted such that the damper would open from the bottom (i.e. the bottom of the damper moves in the direction of the airflow as it opens). We compared temperature stratification for the typical and flipped damper orientations. The results showed that at each damper position, the flipped damper orientation caused less temperature stratification, with the mean deviation from each grid's average temperature being about 2ºF lower than in the same tests ran with the typical damper position. In other words, a single point DAT sensor in the same position would have measured a temperature that is more representative of the true average if the damper is flipped in this one comparison. Additionally, we saw that at more closed damper positions, the flipped

damper caused smaller capacity losses with capacity up to 6% higher when the damper was flipped. For these tests, the maximum uncertainty in capacity measurements was 5.3%. Given that the highest capacity increase was less than 1% higher than the maximum uncertainty, we do not believe the results are conclusive enough to be actionable without further investigation and repeat tests on other box and coil combinations.

## Impact of Insulation

We ran four tests for which we removed the insulation around the coil housing, tube bends, and HWS/R headers. We then repeated these four tests under identical conditions with the coil insulation applied. Comparing the waterside heat transfer for the insulated vs. uninsulated cases, we found that an uninsulated coil showed about 200 BTU/hr (59 W) heat loss. For context, 200 BTU/hr (59 W) is the equivalent rate of heat loss for a 4-foot length of uninsulated ¾" copper pipe at 160ºF (71ºC) under the same ambient conditions as tested. This is relatively small loss when normalized by the capacity of each coil as it is approximately 1% of the coil heating capacity. We also ran three tests for which we left the coil housing, tube bends, and headers uninsulated, as well as control valves and strainers and 10 feet (3 m) of uninsulated ¾" pipe, which is typical of how these systems are commonly installed in the field. We repeated these three tests under identical conditions with the piping, valve body, strainers, headers, coil housing, and tube bends insulated. We found that across these three tests, the maximum heat loss was approximately 750 BTU/hr (220 W) (equivalent to 15 ft (4.6 m) of uninsulated ¾" pipe at 160ºF (71ºC), or 5% of insulated capacity).

Though the heat losses of these tests appear small at the level of a single terminal unit, especially when normalized against the coil's maximum heating capacity, consider them at the whole-building level. The losses will accumulate and the rejected heat enters the return plenum, increasing cooling loads during summer months. For example, a 100k $ft^2$ (9,300 $m^2$) building with 100 boxes, half of which are reheating, would experience the equivalent heat loss of 750 feet (229 m) of uninsulated piping, or 38 kBTU/hr (11 kW) of continuous unnecessary load on the chiller. In other words, these losses from uninsulated piping would both make up a substantial loss of heat to unconditioned space and unnecessarily add to cooling loads when heat is lost to the return plenum. We therefore recommend that coil and valve train insulation be applied in new construction projects and that in retrofit projects, coil insulation should be applied along with other VAV box measures (e.g. repairs, box replacement, etc.).

## Field Installation and Operation Methods

A common challenge encountered in the field is when site conditions and supply constraints force installers to install right-handed coils in a left-handed orientation (or vice-versa). One of two solutions to this challenge is typically employed. The first, incorrect, solution is to connect the HWS piping at the bottom of the coil as usual, resulting in parallel flow of water through the coil. The other, correct, solution is to connect the HWS piping at the top of the coil, resulting in counter flow through the coil. Through discussions with various designers, manufacturers, and contractors, we have found that connecting the HWS at the bottom of the coil is the most common method used as installers have typically been trained to 'always supply from the bottom'. The justification for supplying from the bottom (as opposed to piping

for counterflow) is grounded in speculation that water flowing from top to bottom will result in trapped air bubbles that negatively impact water flow and heat transfer. However, we have found through the same conversations that there is no known data or reasonable theory to support these claims.

To demonstrate the impact of using one method over the other, we ran two tests with the HWS connected at the bottom of the coil in one and at the top of the coil in the other, but otherwise the tests were identical (12" box, 3-row coil, 120ºF HWST). The measured waterside heat transfer for both tests shows that connecting the HWS piping at the bottom of the inverted coil (i.e. parallel flow) reduced capacity by 2.5 MBH (0.73 MW) (10%) compared to counter flow. This decrease in capacity is significant enough to justify the use of the counter flow piping method even when a coil with the incorrect handing is encountered as best practice in coil installation. We therefore recommend that this method be codified required installation practice in applicable energy codes.

We also ran two tests in which we shut off airflow and only kept water flowing through the coil. We ran one test with 160ºF (71ºC) and the other with 120ºF (49ºC) HWST. This was to simulate zone control systems which are commonly operated with hot water continuously flowing through the coil even while the zone is unoccupied and the air handlers are off (i.e. there is no forced air flow through the coil). For the 160ºF (71ºC) HWST test, the coil capacity was about 2.1 kBTU/hr (0.61 kW) while for the 120ºF (49ºC) HWST test, it was about 1.3 kBTU/hr (0.38 kW). Both of these measured capacities represent about 7% of their respective design capacities as determined by the AHRI 410 certified modeling software. This would represent a significant loss of heating energy on a whole building level in buildings employing this type of airside zone control with poor or overridden waterside controls. We therefore recommend that buildings using zone control systems ensure that the airside controls are coupled with waterside controls at each terminal unit and that VAV box coil valves do not operate unless both the heat plant and air handler are operating.

## Impact of Coil Circuiting

We designed four custom coils which we tested as part of the same experiments. Each custom design focused on changing the circuiting from their typical counterparts, to either enable more symmetrical heat distribution (decrease stratification) and left/right symmetry (for avoiding installation issues) or enable higher hot water temperature changes (increase capacity through higher waterside temperature differences ("delta T") at low HWST). We present a sketch of our designs in Figure 6.

## Figure 6: Custom Coil Designs

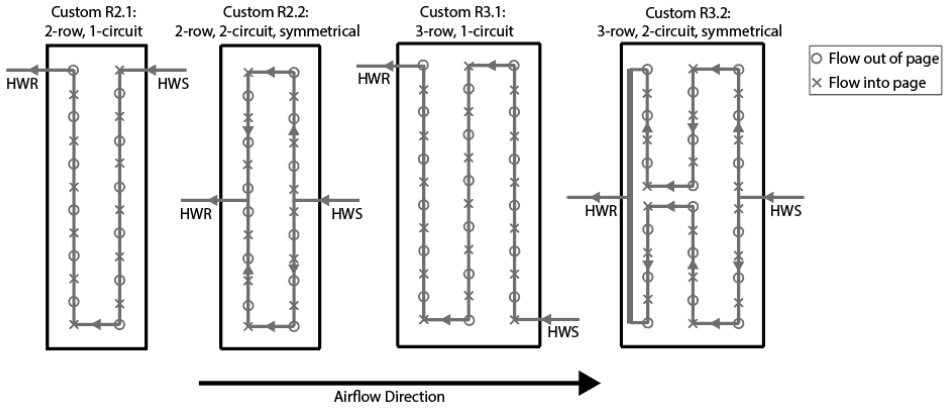


**Circuiting diagram of custom coils. Note the nomenclature of the design names: "R[rows].[circuits]"**

Our results showed that these custom coils lost capacity at similar rates to their typical counterparts as the damper closed. However, the total capacity of the custom coils was mostly higher than or nearly identical to that of their typical counterparts. As we maintained identical air and water flow through the coils, we saw an identical trend of increasing waterside temperature difference (i.e. higher waterside "Delta T"). The total capacity of the custom coils was higher than typical coils particularly at 120ºF HWST (Figure 7) at least in this limited set of three comparisons.

## Figure 7: Custom Coil Capacities

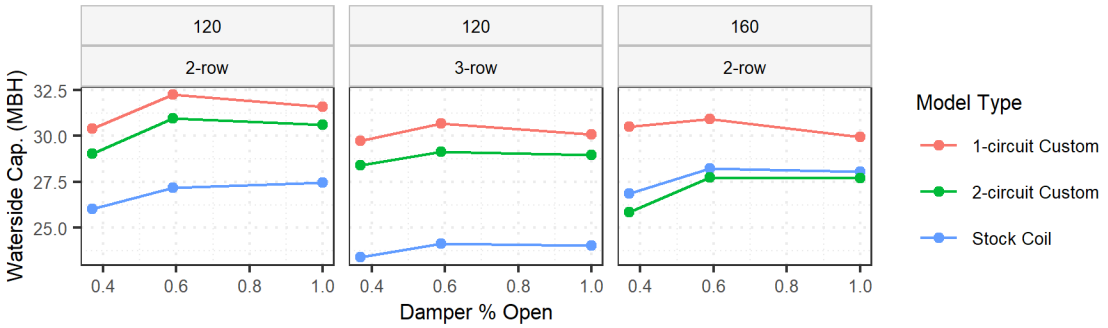


**Change in total capacity with damper position. Grouped by HWST and number of coil rows.**

We also collected results on discharge air temperature stratification for the custom coils. We expected the coils with symmetrical circuiting (Custom R2.2, Custom R3.2) to slightly improve stratification. However, our results showed that the only condition for which stratification was meaningfully reduced by the custom coils was at 120ºF (49ºC) HWST with a 2-row coil. Otherwise, these coils did not make any discernible impact on stratification during the tests we ran, with stratification even slightly increasing for some tests (Figure 8). While the custom coils did not impact temperature stratification, our results show, once again (see Figure 4b), that stratification tends to increase with more closed damper positions. This suggests that damper position, more so than other aspects of coil design, is a strong driver of temperature stratification in VAV HW reheat systems.

**Figure 8: Custom Coil Temperature Stratification**

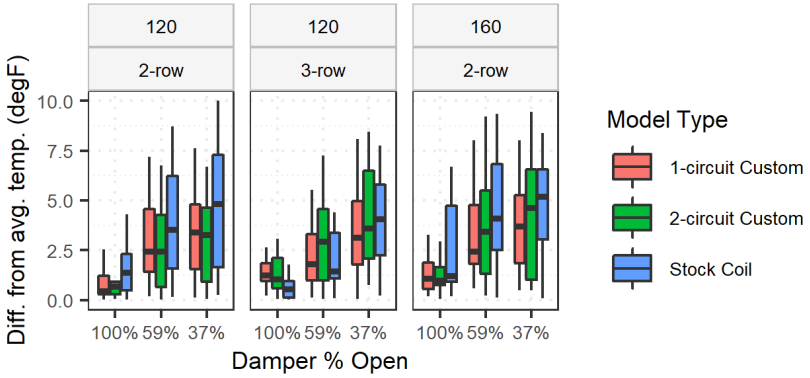


**Discharge air temperature stratification typical vs. custom coils. Grouped by HWST and number of coil rows.**

Though stratification is not markedly improved by the custom coils, our results indicate that increases in coil capacity can be attained with a simple change in circuiting alone. The use of symmetrical circuiting (Custom R2.2, Custom R3.2) provides the additional benefit of preventing performance deficits due to field installation errors with single-handed coils (see previous section on field installation methods) while also providing increased capacities and waterside temperature drops at low HWST. This performance benefit will allow buildings pursuing design HWST decreases (i.e. 160ºF (71ºC) to 120ºF (49ºC)) to limit the increases in pumping energy and/or forego costly pipe size increases that would otherwise be required if the coil design were to remain unchanged. We therefore recommend that coil manufacturers allocate additional resources to exploring and potentially improving coil circuiting designs for terminal unit hot water heating coils. While our own custom designs were shown to have improved performance relative to the typical coils, our results represent only a brief examination of the issue. This warrants further investigation into whether more optimal circuiting designs than typical can be realized.

# CHAPTER 4: Conclusions

Our results reveal that damper position significantly impacts leaving air temperature stratification and coil capacity when airflow through the coil remains constant. We additionally showed that at 100% open damper positions, predictions from coil selection software are accurate even at lower than design HWST. Our results measured the losses from the uninsulated valve train, piping, and coil frame and bends, and measured the losses from coils without forced airflow through the VAV box. Based on our results, we recommend:

1. Designers should use static pressure reset sequences in VAV reheat systems to minimize capacity losses at more closed damper positions (in addition to fan energy savings). For boxes close to air handlers, consider installing manual balancing dampers to reduce the static pressure that the VAV box damper must decrease when it limits airflow to the design heating airflow setpoint.
2. Designers should mount single-point DAT sensors as close to the centerline of the duct as possible, as far from the coil as possible.
3. Designers and builders in new construction projects should insulate all valves, pipes, coil components and housing, while in retro-fits, these should be insulated at the same time as other VAV box measures.
4. Any applicable guidance (e.g. from manufacturer documents, energy codes, etc.) should incorporate the requirement for installers to maintain counter flow in all coil installations, even where site conditions prevent installation in the originally-designed handedness. Distributors could play a role in preventing on-site installation errors by stocking both left- and right-handed coils to provide the proper coil for any field condition.
5. For all buildings using zone-based occupancy controls, designers should ensure that both airside and waterside controls are employed to avoid energy losses during unoccupied hours.
6. Coil manufacturers should allocate additional resources to re-designing typical coil circuiting, with a focus on symmetry to avoid performance deficits due to incorrect field installation and/or limited circuits to increase waterside temperature differences for low HWST.
7. Designers can rely on coil selection software to estimate capacities at low design water temperatures, both for new construction and in retrofit applications.

# REFERENCES


*ASHRAE Guideline 36-2021 High-Performance Sequences of Operation for HVAC Systems*. (2021). ASHRAE.

Edward Arens, Hui Zhang, Tyler Hoyt, Soazig Kaam, John Goins, & Fred Bauman. (2012). *Thermal air quality acceptability in buildings that reduce energy by reducing minimum airflow from overhead diffusers. Final report for ASHRAE RP-1515.* ASHRAE.

Raftery, P., Geronazzo, A., Cheng, H., & Paliaga, G. (2018). Quantifying energy losses in hot water reheat systems. *Energy and Buildings*, *179*, 183–199.

Steve Taylor. (2015). VAV Box Duct Design. *ASHRAE Journal*, *July 2015*, 32–38.

Steve Taylor & Jeff Stein. (2004). Sizing VAV Boxes. *ASHRAE Journal*, *March 2004*, 30–34.

Wendler, P., Raftery, P., & Cheng, H. (2023, February 5). VAV HW Reheat Terminal Units: Temperature Stratification, Performance at Low HWST, and Myths from the Field. *CPS 6: Case Studies on Performance and Losses in Hydronic, VAV and Heat Pump Systems*. 2023 ASHRAE Winter Conference, Atlanta, GA.

# APPENDIX A:
# Discharge Air Temperature Stratification Box Plots

Notes:

- Temperature stratification by box size, coil rows, and HWST.
- Temperature differences shown are in absolute units.

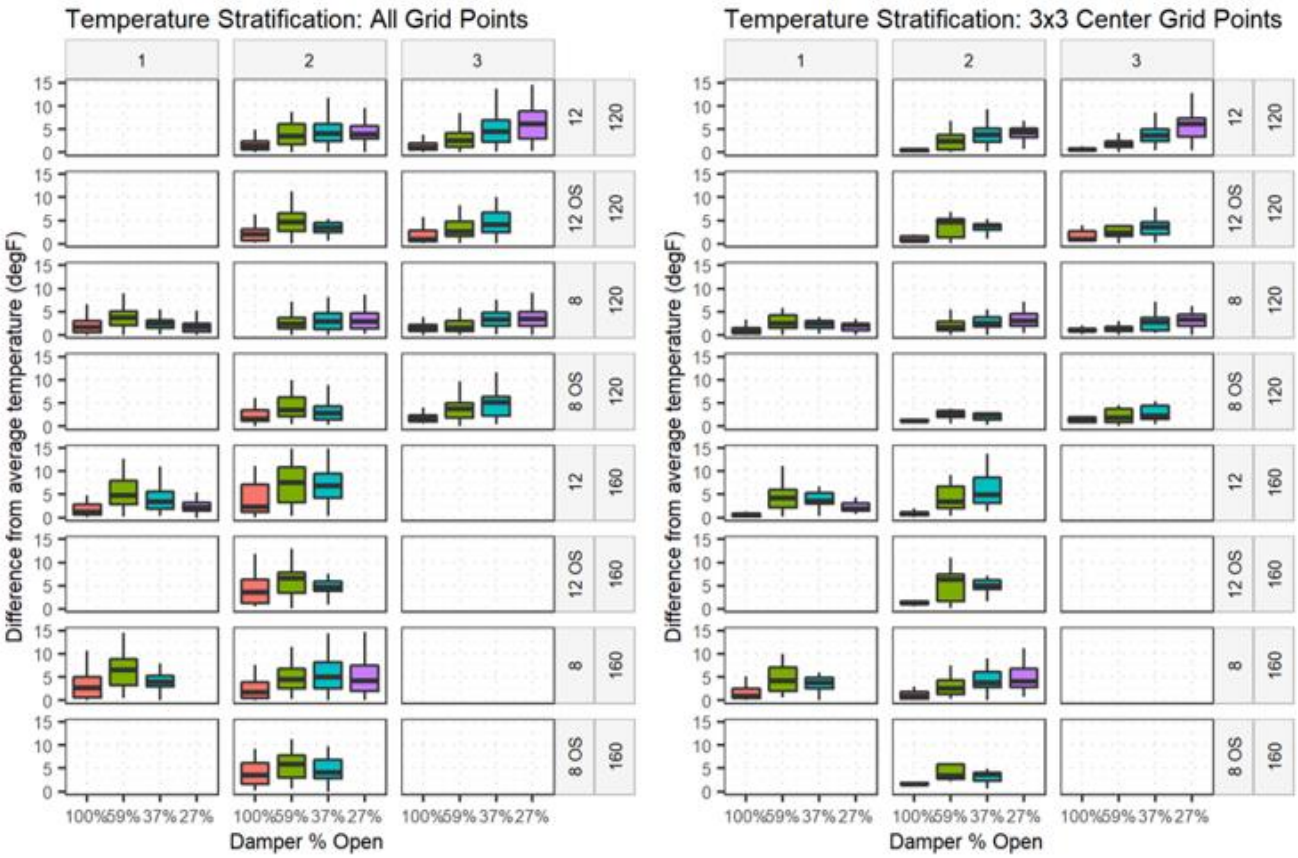

# APPENDIX B:
# Discharge Air Temperature Stratification Heatmaps

Notes:

- Each heatmap shows the average percent difference between the average temperature measured in the plenum and the point temperature averaged for each thermocouple couple position averaged across all three thermocouple grids.
- Test ID nomenclature is as follows: [test order #]:[box size (in.)]:[coil rows]:[HWST (ºF)]:[damper % open]
    - Test ID **100:12:2:120:59%** therefore indicates the **100th** test in the experiment, ran with a **12" box**, a **2-row coil**, at **120ºF HWST**, with the damper **59% open**.
- Damper was flipped for test order # 035 – 038.
- The inverted 3-row left-handed coil was used in test order # 018 (HWS connected at top of coil) and test order # 019 (HWS connected at bottom of coil).
- Custom coils were used in test order # 090 – 107.
    - 1-circuit 2-row coil: test order # 090 – 095.
    - 2-circuit 2-row coil: test order # 096 – 101.
    - 1-circuit 3-row coil: test order # 102 – 104.
    - 2-circuit 3-row coil: test order # 105 – 107.

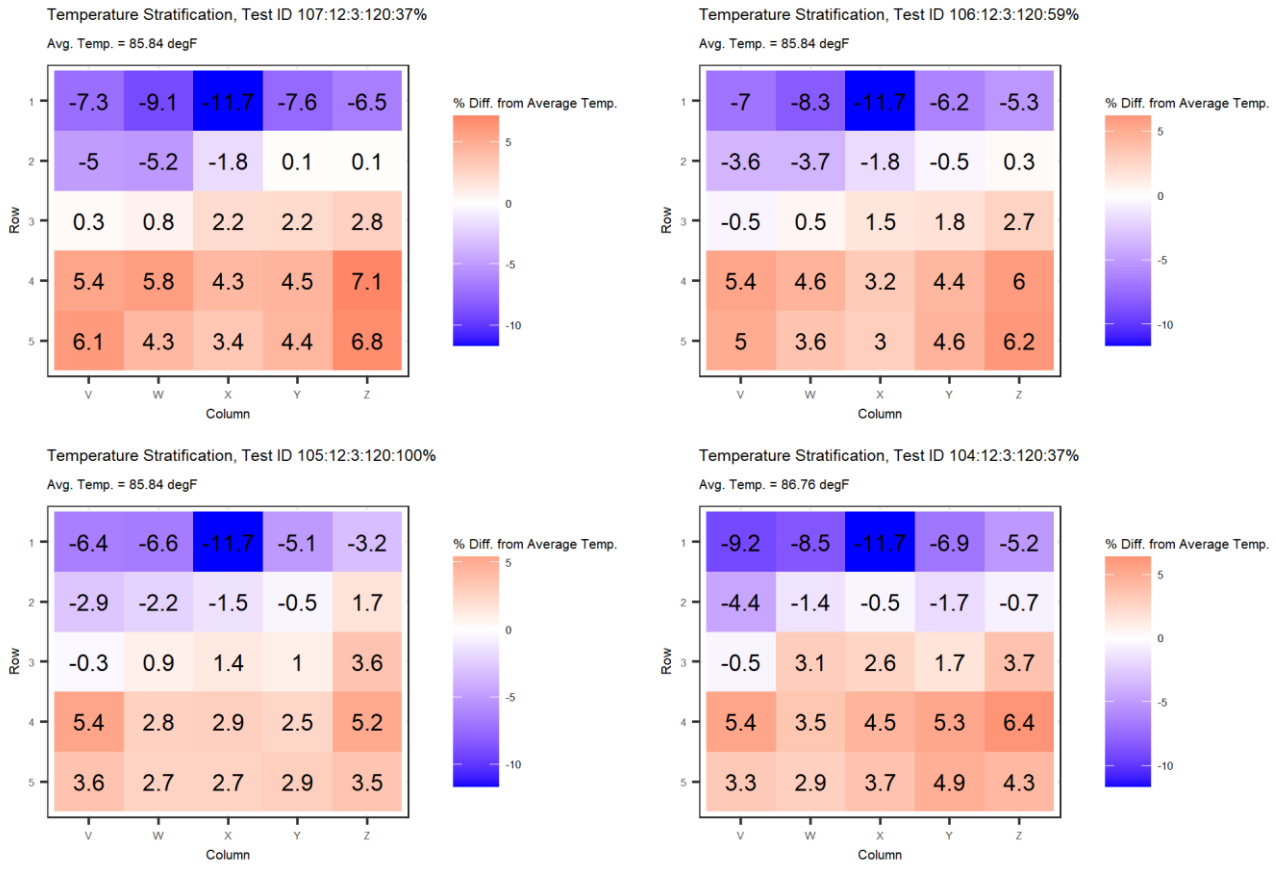

Temperature Stratification, Test ID 103:12:3:120:59%

Avg. Temp. = 86.76 degF

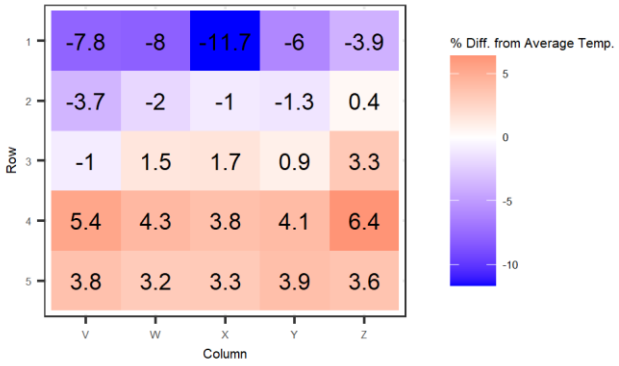


Temperature Stratification, Test ID 102:12:3:120:100%

Avg. Temp. = 87.68 degF

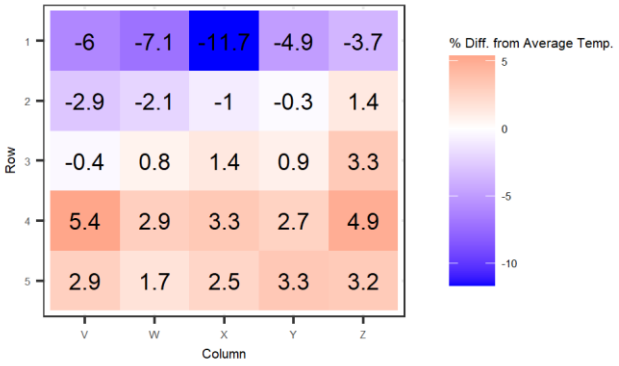


Temperature Stratification, Test ID 101:12:2:120:37%

Avg. Temp. = 85.84 degF

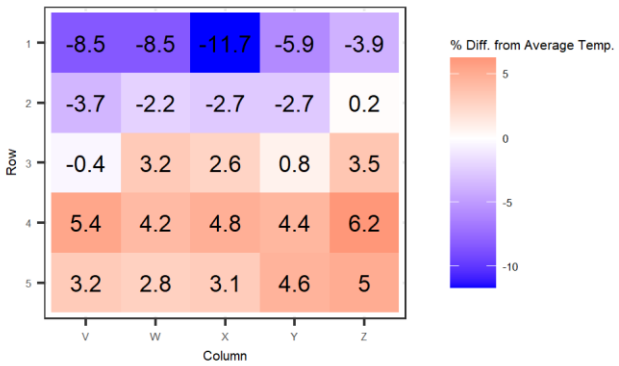


Temperature Stratification, Test ID 100:12:2:120:59%

Avg. Temp. = 85.84 degF

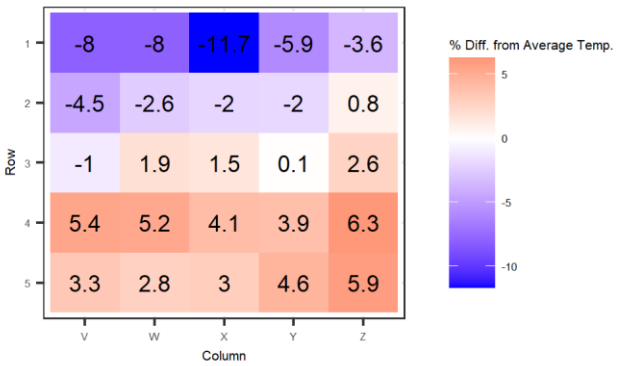


Temperature Stratification, Test ID 099:12:2:120:100%

Avg. Temp. = 86.76 degF

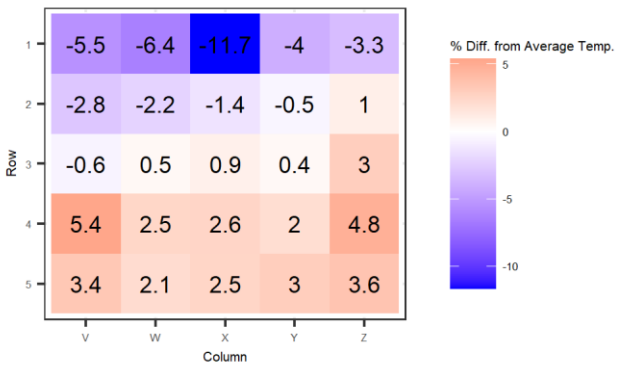


Temperature Stratification, Test ID 098:12:2:160:37%

Avg. Temp. = 86.76 degF

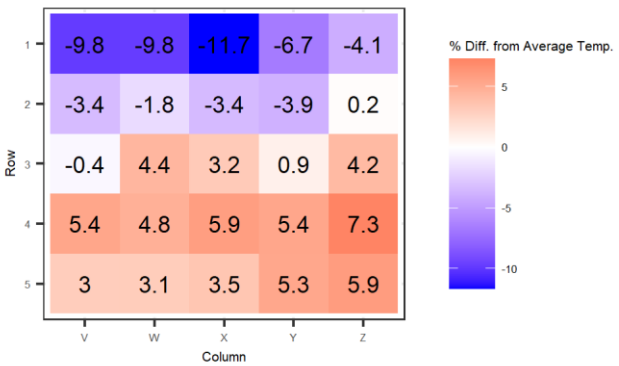


Temperature Stratification, Test ID 097:12:2:160:59%

Avg. Temp. = 85.84 degF

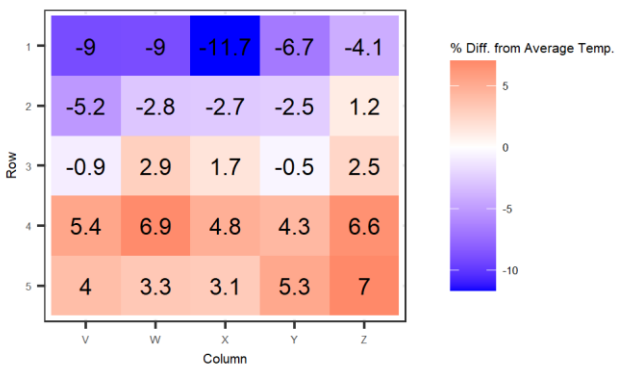


Temperature Stratification, Test ID 096:12:2:160:100%

Avg. Temp. = 86.76 degF

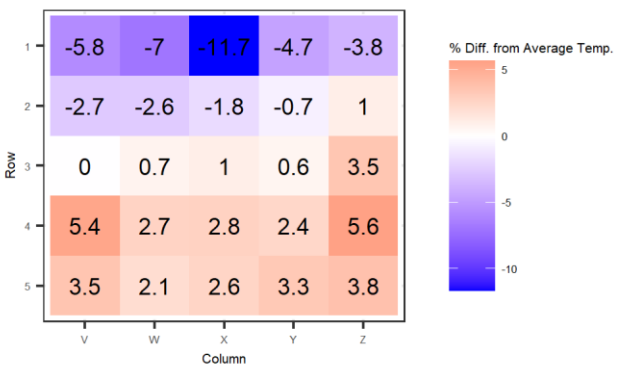

Temperature Stratification, Test ID 095:12:2:160:37%

Avg. Temp. = 88.6 degF

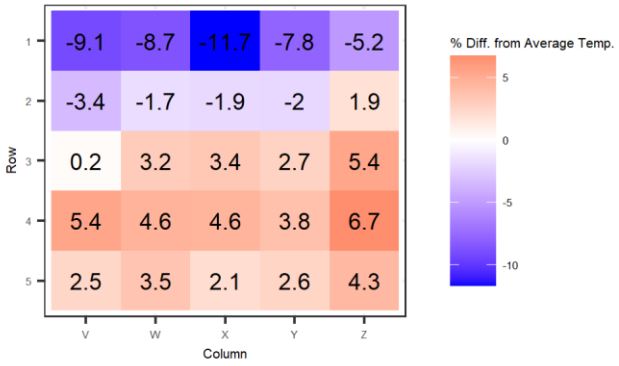


Temperature Stratification, Test ID 094:12:2:160:59%

Avg. Temp. = 89.52 degF

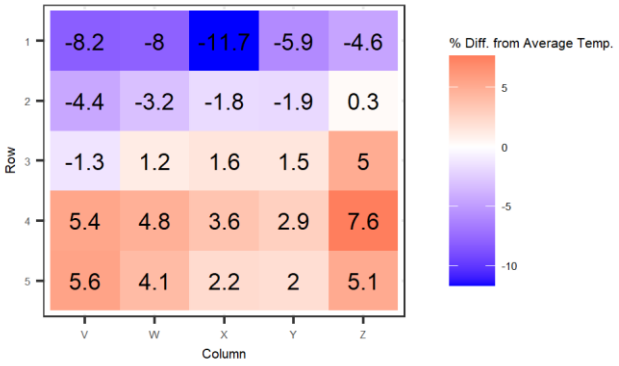


Temperature Stratification, Test ID 093:12:2:160:100%

Avg. Temp. = 89.52 degF

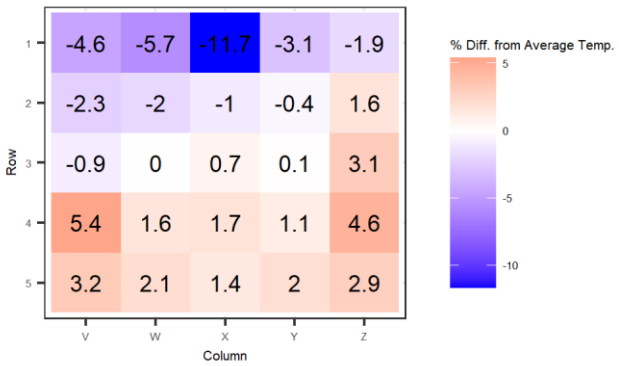


Temperature Stratification, Test ID 092:12:2:120:37%

Avg. Temp. = 86.76 degF

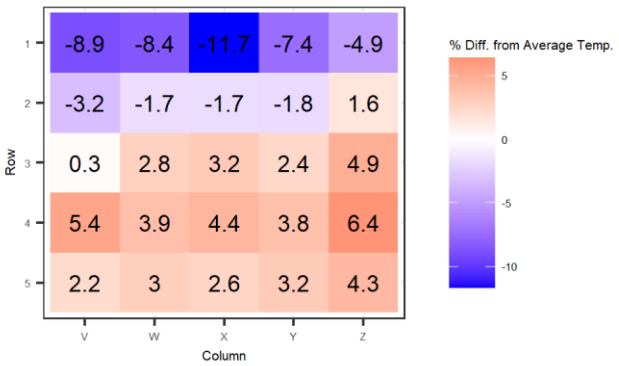


Temperature Stratification, Test ID 091:12:2:120:59%

Avg. Temp. = 86.76 degF

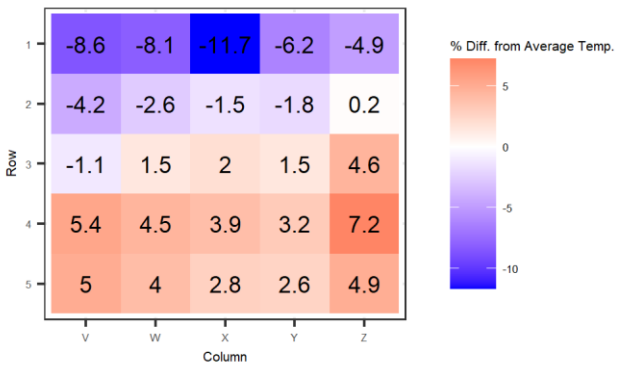


Temperature Stratification, Test ID 090:12:2:120:100%

Avg. Temp. = 87.68 degF

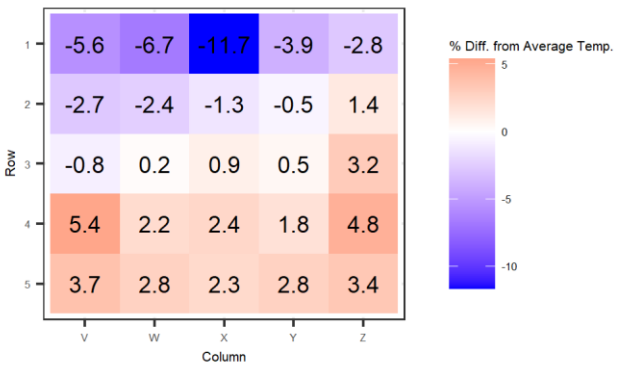


Temperature Stratification, Test ID 089:12:2:160:37%

Avg. Temp. = 86.76 degF

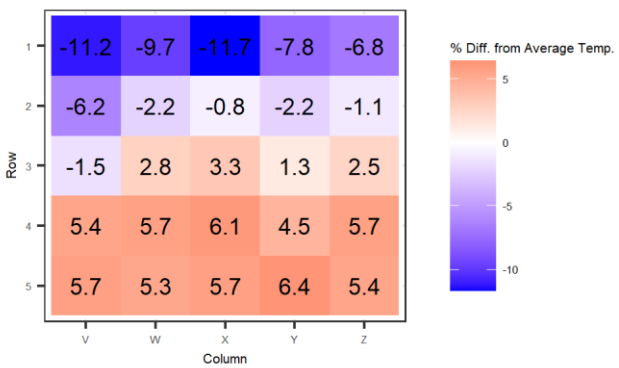


Temperature Stratification, Test ID 088:12:2:160:59%

Avg. Temp. = 86.76 degF

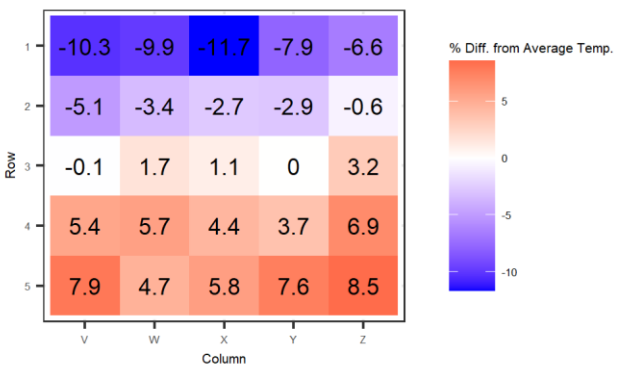

Temperature Stratification, Test ID 087:12:2:160:100%

Avg. Temp. = 86.76 degF

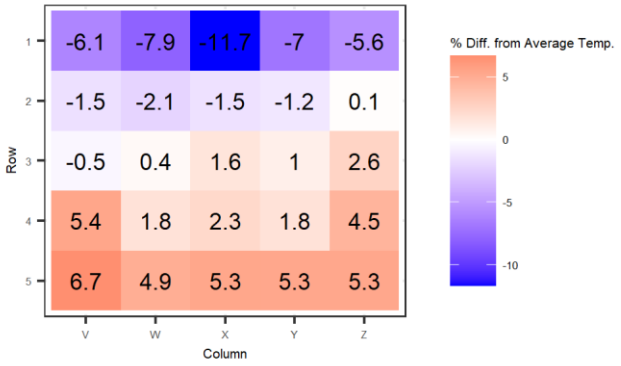


Temperature Stratification, Test ID 086:12:2:120:37%

Avg. Temp. = 80.32 degF

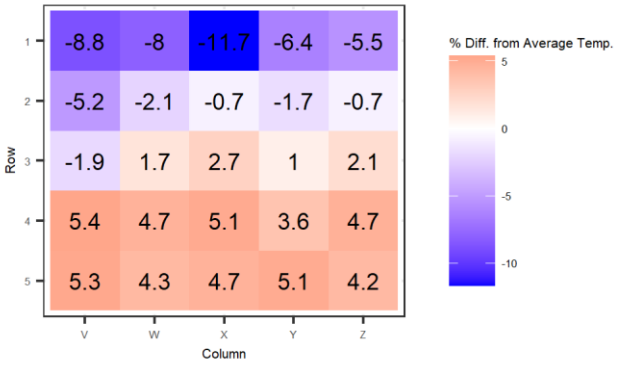


Temperature Stratification, Test ID 085:12:2:120:59%

Avg. Temp. = 80.32 degF

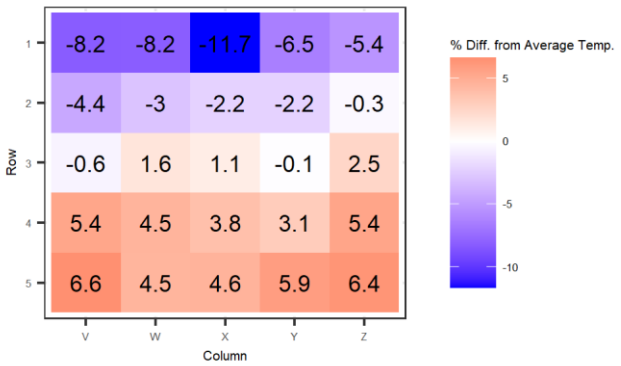


Temperature Stratification, Test ID 084:12:2:120:100%

Avg. Temp. = 81.24 degF

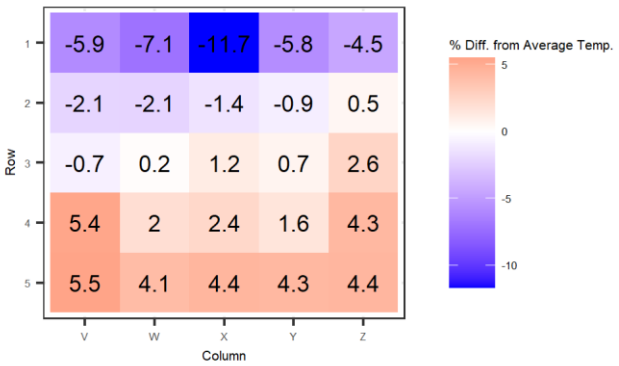


Temperature Stratification, Test ID 083:12:3:120:37%

Avg. Temp. = 84 degF

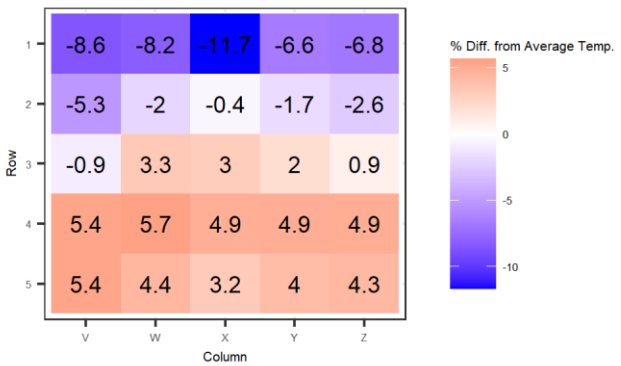


Temperature Stratification, Test ID 082:12:3:120:59%

Avg. Temp. = 84 degF

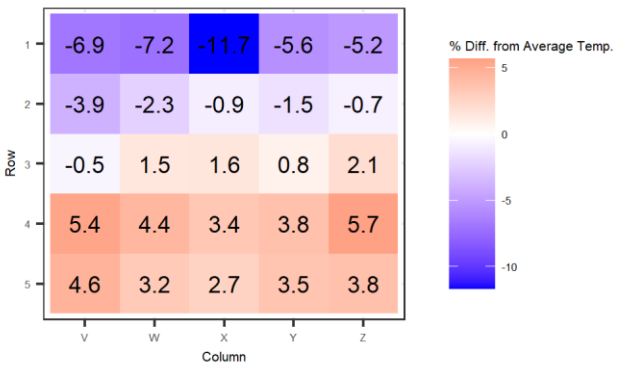


Temperature Stratification, Test ID 081:12:3:120:100%

Avg. Temp. = 84 degF

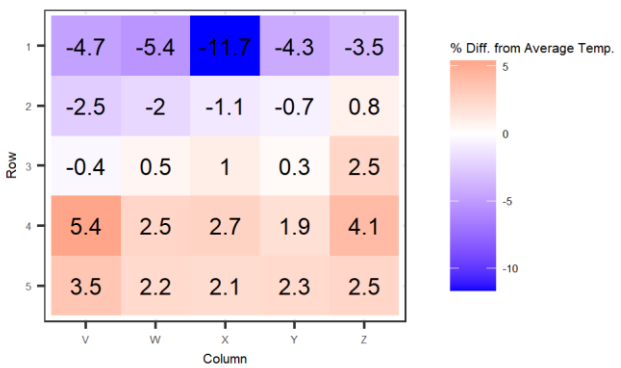


Temperature Stratification, Test ID 080:12:1:160:37%

Avg. Temp. = 84 degF

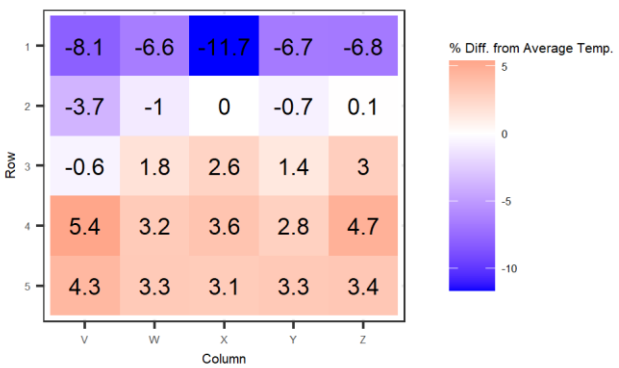

Temperature Stratification, Test ID 079:12:1:160:59%

Avg. Temp. = 84.92 degF

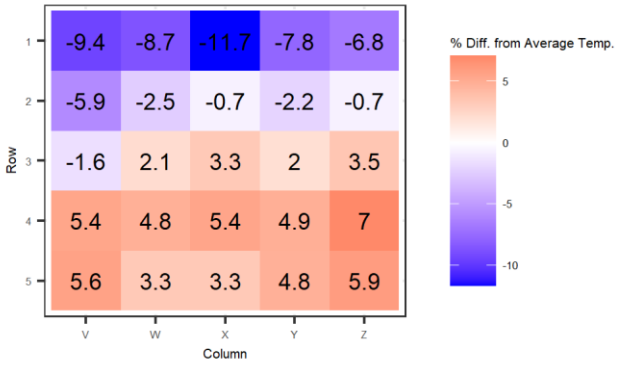


Temperature Stratification, Test ID 078:12:1:160:100%

Avg. Temp. = 84.92 degF

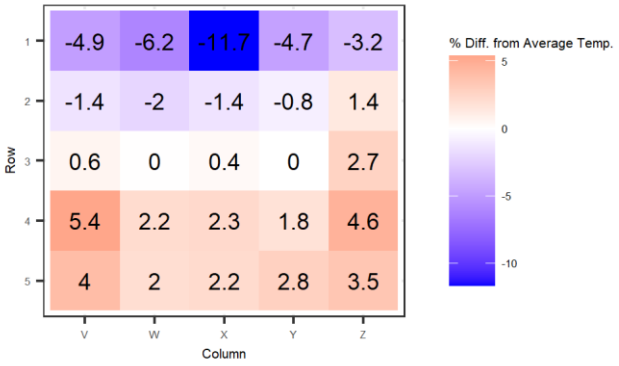


Temperature Stratification, Test ID 077:8 OS:3:120:37%

Avg. Temp. = 84 degF

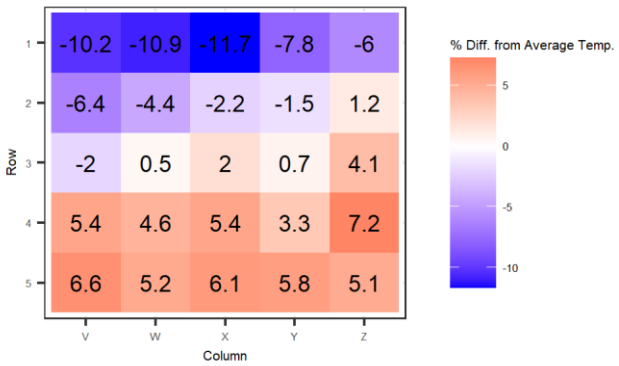


Temperature Stratification, Test ID 076:8 OS:3:120:59%

Avg. Temp. = 86 degF

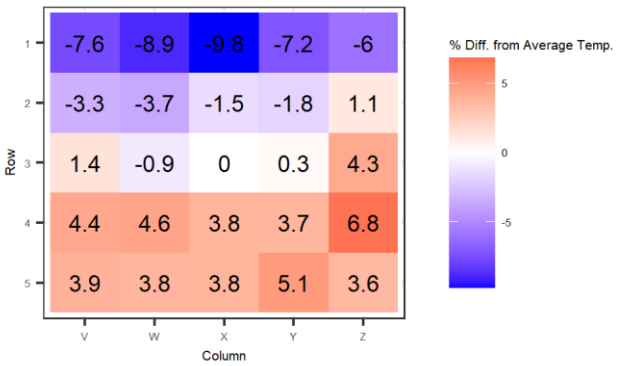


Temperature Stratification, Test ID 075:8 OS:3:120:100%

Avg. Temp. = 86 degF

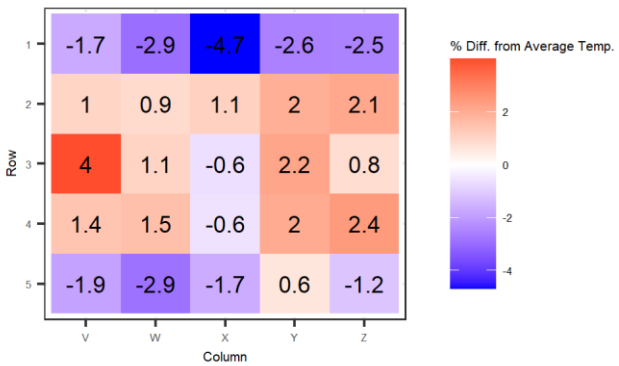


Temperature Stratification, Test ID 074:8 OS:2:120:37%

Avg. Temp. = 85 degF

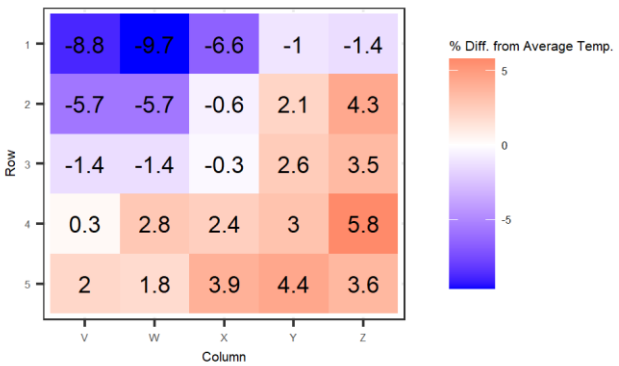


Temperature Stratification, Test ID 073:8 OS:2:120:59%

Avg. Temp. = 88 degF

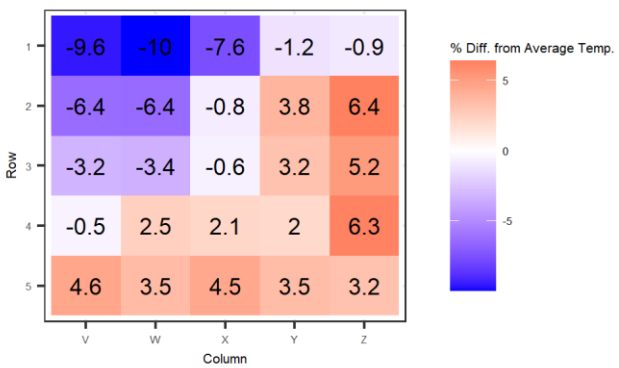


Temperature Stratification, Test ID 072:8 OS:2:120:100%

Avg. Temp. = 88 degF

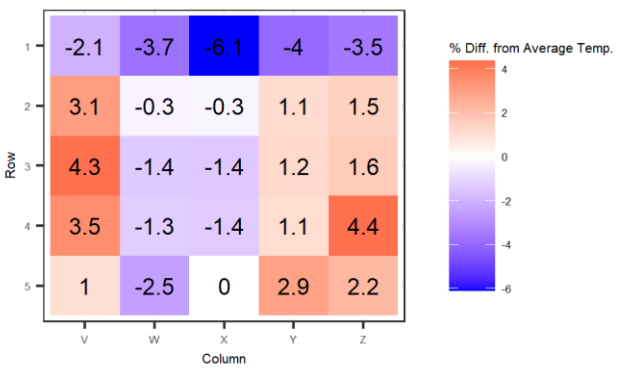

Temperature Stratification, Test ID 071:8 OS:2:160:37%

Avg. Temp. = 86 degF

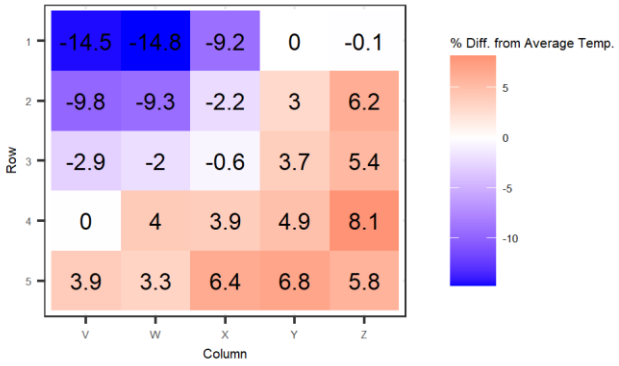


Temperature Stratification, Test ID 070:8 OS:2:160:59%

Avg. Temp. = 90 degF

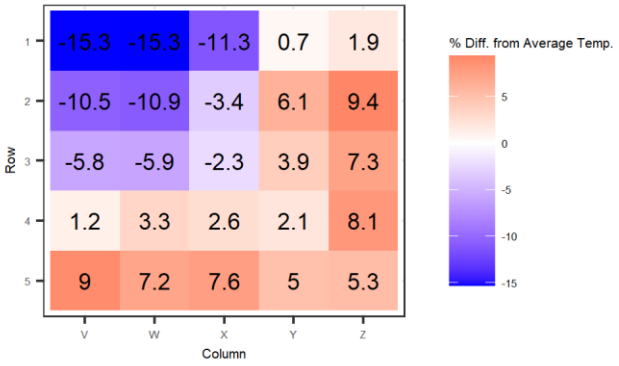


Temperature Stratification, Test ID 069:8 OS:2:160:100%

Avg. Temp. = 90 degF

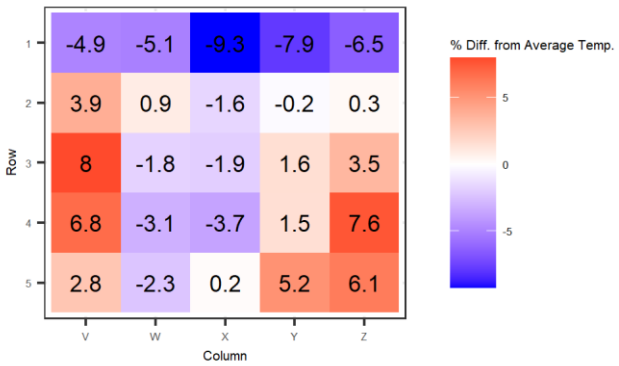


Temperature Stratification, Test ID 068:12 OS:3:120:37%

Avg. Temp. = 88 degF

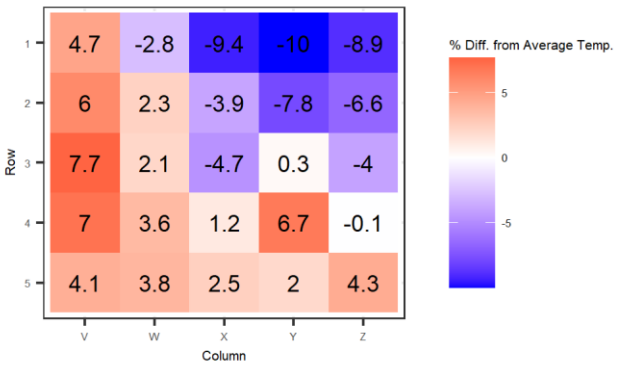


Temperature Stratification, Test ID 067:12 OS:3:120:59%

Avg. Temp. = 88 degF

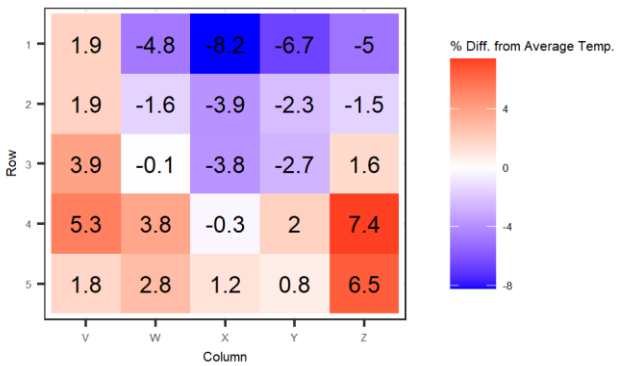


Temperature Stratification, Test ID 066:12 OS:3:120:100%

Avg. Temp. = 88 degF

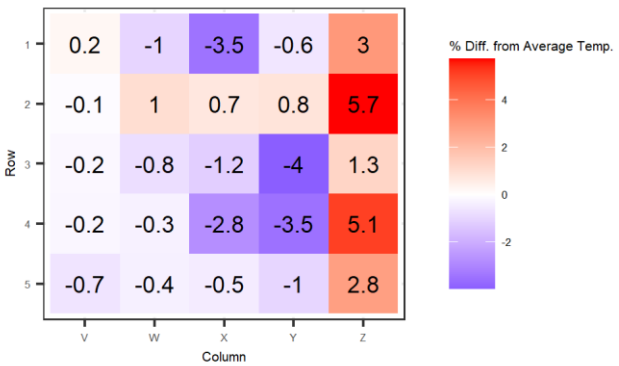


Temperature Stratification, Test ID 065:12 OS:2:120:37%

Avg. Temp. = 86 degF

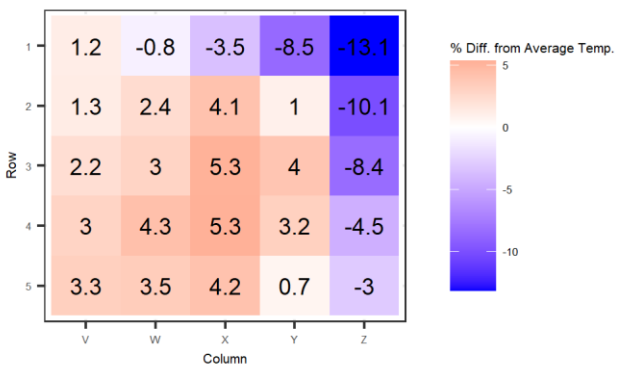


Temperature Stratification, Test ID 064:12 OS:2:120:59%

Avg. Temp. = 90 degF

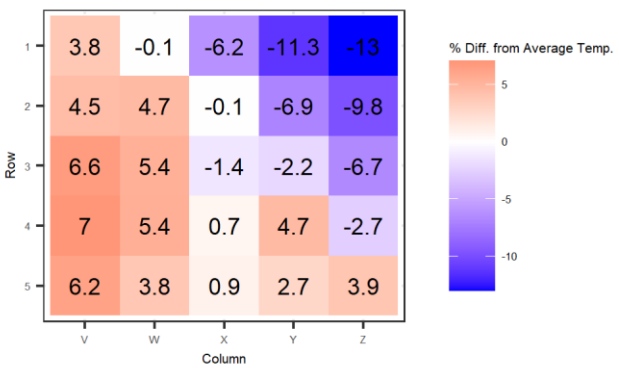

Temperature Stratification, Test ID 063:12 OS:2:120:100%

Avg. Temp. = 89 degF

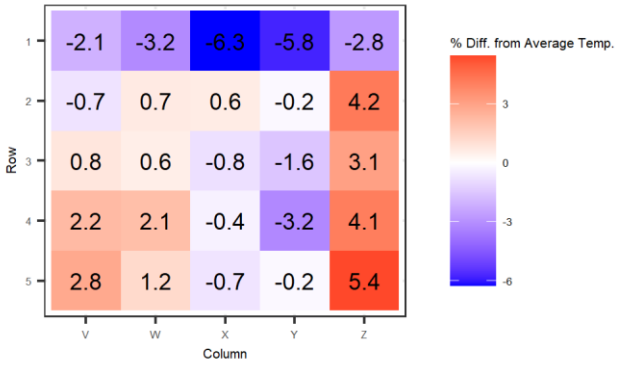


Temperature Stratification, Test ID 062:12 OS:2:160:37%

Avg. Temp. = 87 degF

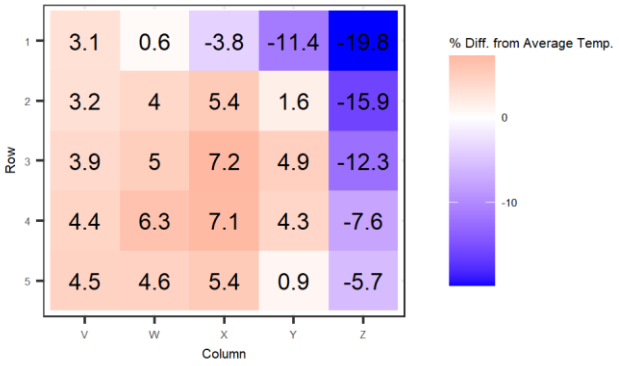


Temperature Stratification, Test ID 061:12 OS:2:160:59%

Avg. Temp. = 92 degF

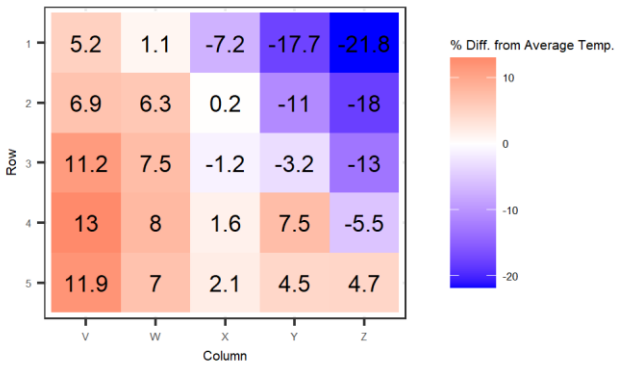


Temperature Stratification, Test ID 060:12 OS:2:160:100%

Avg. Temp. = 91 degF

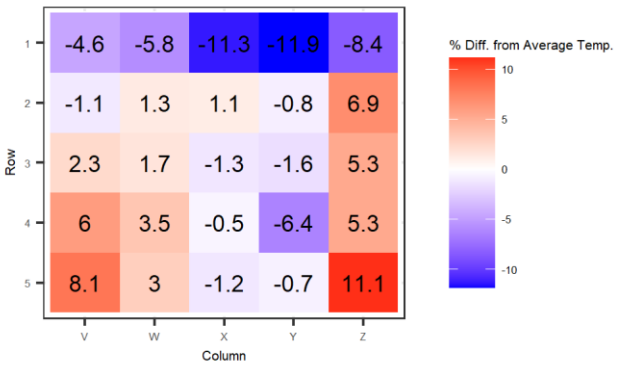


Temperature Stratification, Test ID 059:8:3:120:27%

Avg. Temp. = 87 degF

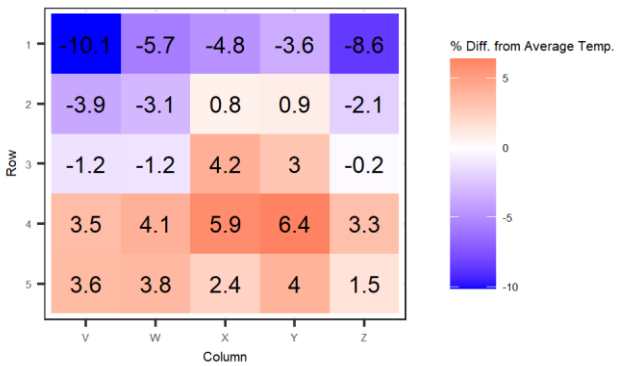


Temperature Stratification, Test ID 058:8:3:120:37%

Avg. Temp. = 87 degF

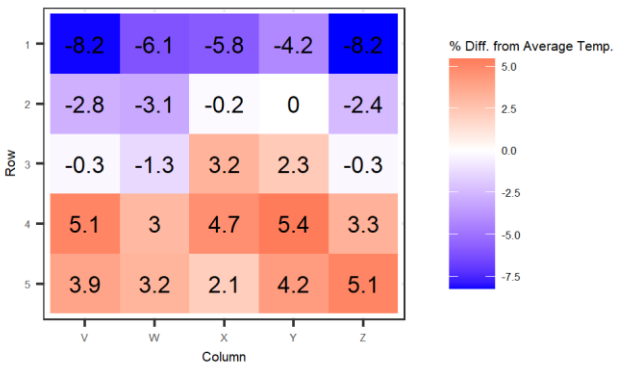


Temperature Stratification, Test ID 057:8:3:120:59%

Avg. Temp. = 87 degF

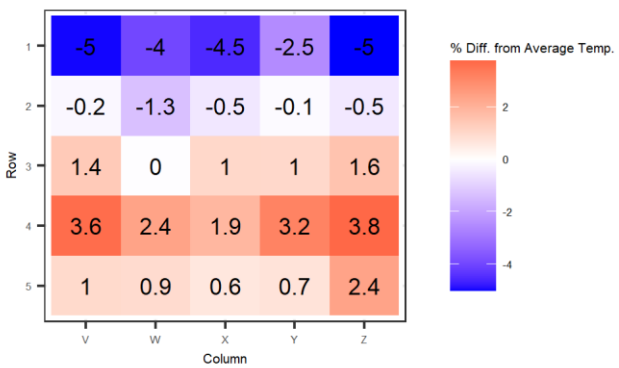


Temperature Stratification, Test ID 056:8:3:120:100%

Avg. Temp. = 87 degF

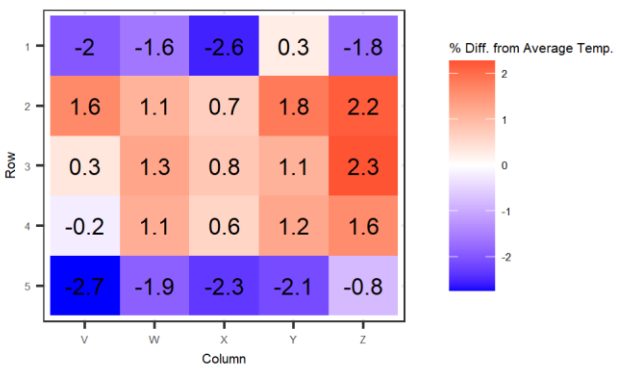

Temperature Stratification, Test ID 052:8:2:120:27%

Avg. Temp. = 84 degF

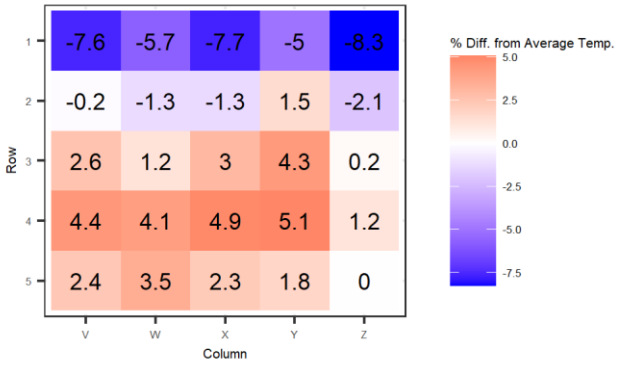


Temperature Stratification, Test ID 051:8:2:120:37%

Avg. Temp. = 85 degF

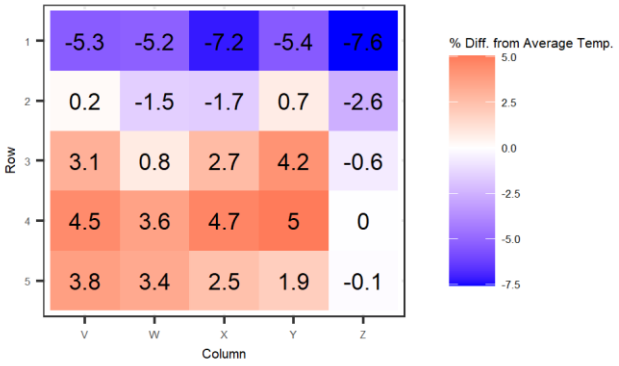


Temperature Stratification, Test ID 050:8:2:120:59%

Avg. Temp. = 86 degF

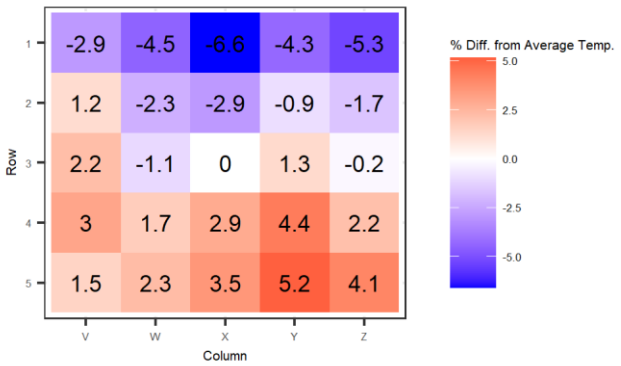


Temperature Stratification, Test ID 047:8:2:160:27%

Avg. Temp. = 85 degF

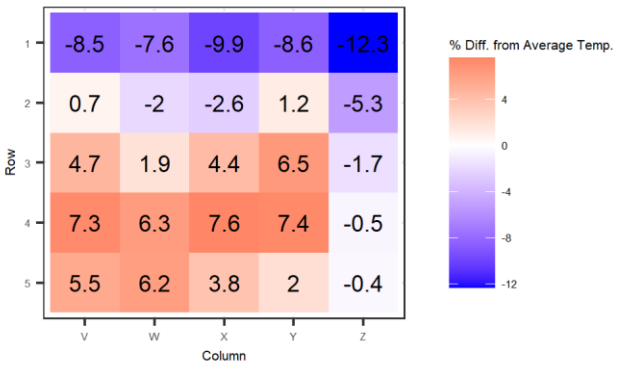


Temperature Stratification, Test ID 046:8:2:160:37%

Avg. Temp. = 87 degF

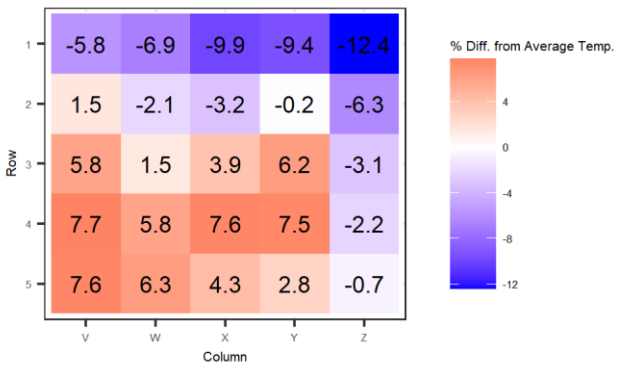


Temperature Stratification, Test ID 045:8:2:160:59%

Avg. Temp. = 87 degF

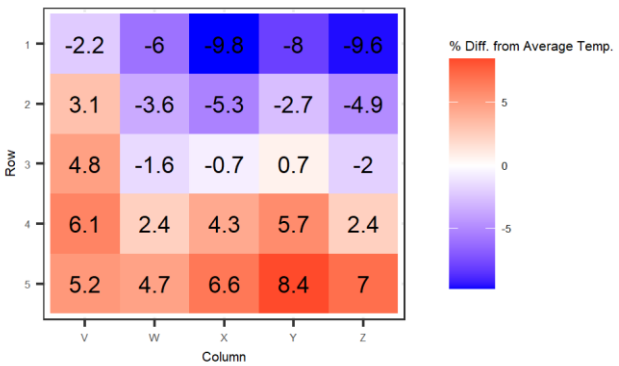


Temperature Stratification, Test ID 044:8:2:160:100%

Avg. Temp. = 87 degF

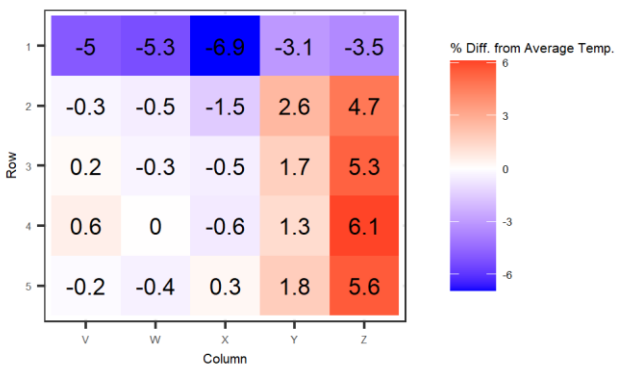


Temperature Stratification, Test ID 042:8:1:120:27%

Avg. Temp. = 76.92 degF

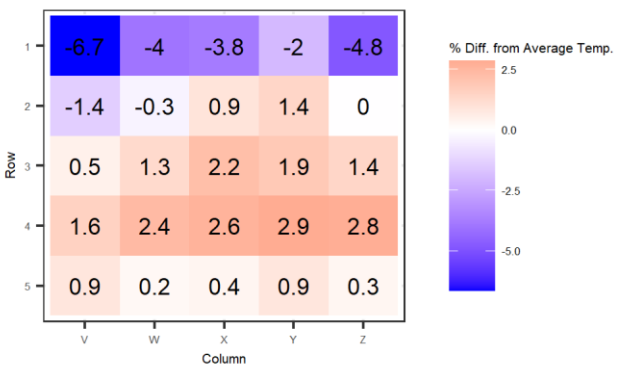

Temperature Stratification, Test ID 041:8:1:120:37%

Avg. Temp. = 75.92 degF

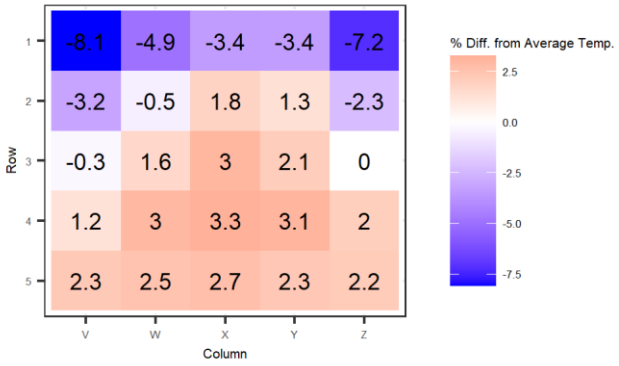


Temperature Stratification, Test ID 040:8:1:120:59%

Avg. Temp. = 77.92 degF

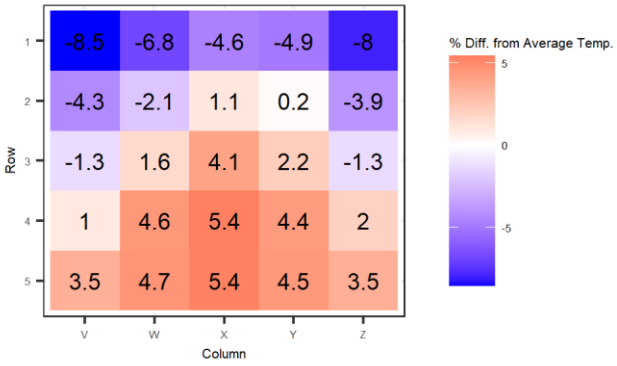


Temperature Stratification, Test ID 039:8:1:120:100%

Avg. Temp. = 77 degF

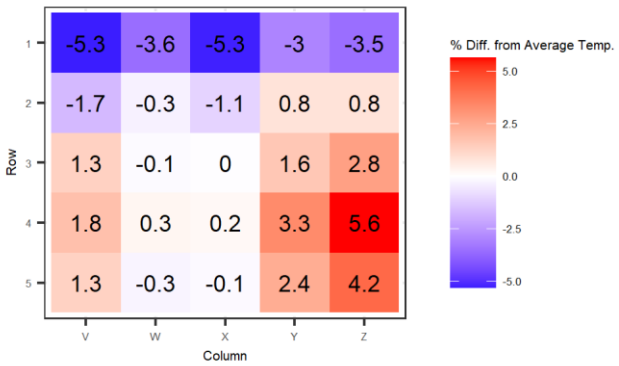


Temperature Stratification, Test ID 038:8:1:160:27%

Avg. Temp. = 87 degF

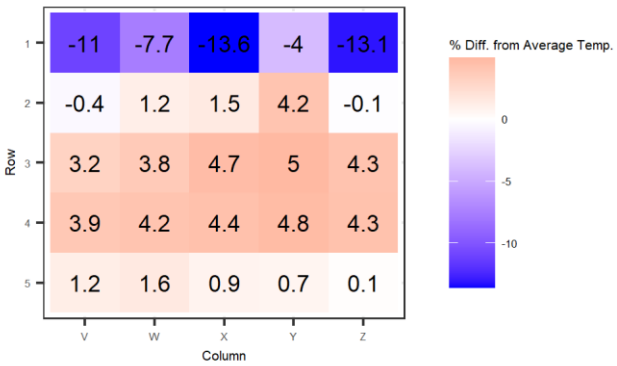


Temperature Stratification, Test ID 037:8:1:160:37%

Avg. Temp. = 88 degF

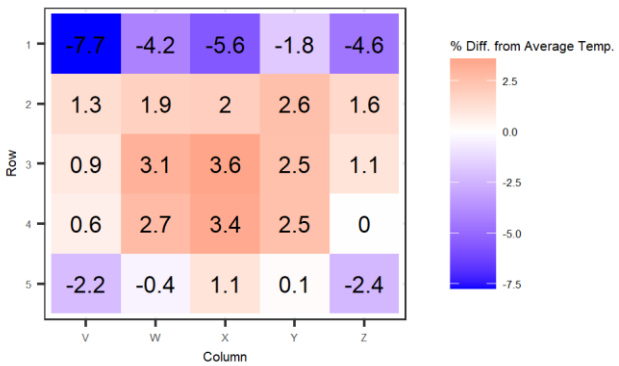


Temperature Stratification, Test ID 036:8:1:160:59%

Avg. Temp. = 90 degF

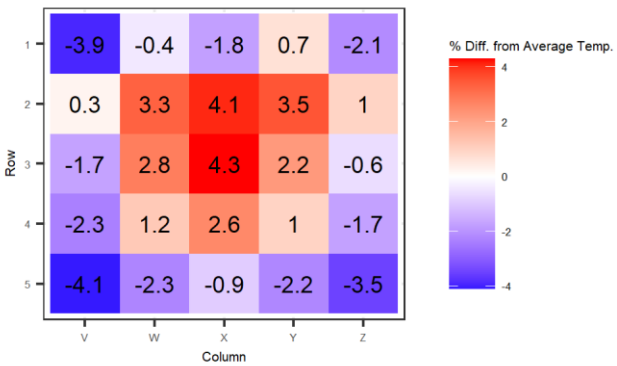


Temperature Stratification, Test ID 035:8:1:160:100%

Avg. Temp. = 89.92 degF

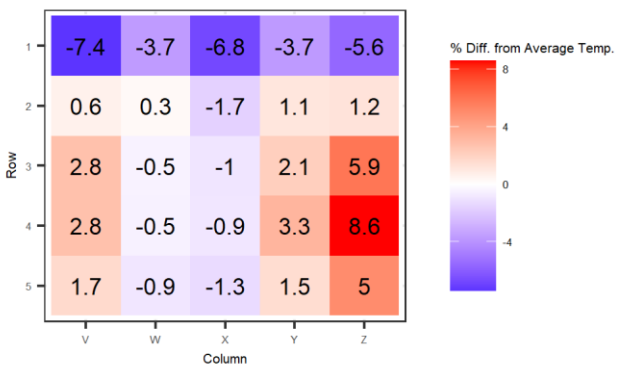


Temperature Stratification, Test ID 034:8:1:160:27%

Avg. Temp. = 87.92 degF

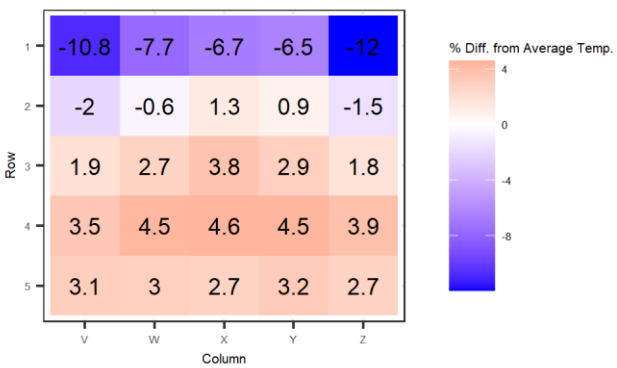

Temperature Stratification, Test ID 033:8:1:160:37%

Avg. Temp. = 86.92 degF

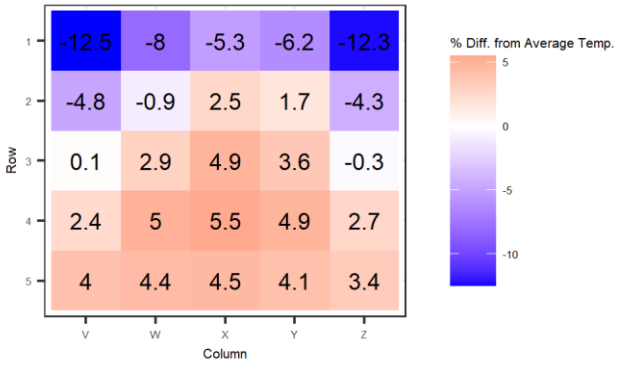


Temperature Stratification, Test ID 032:8:1:160:59%

Avg. Temp. = 89.92 degF

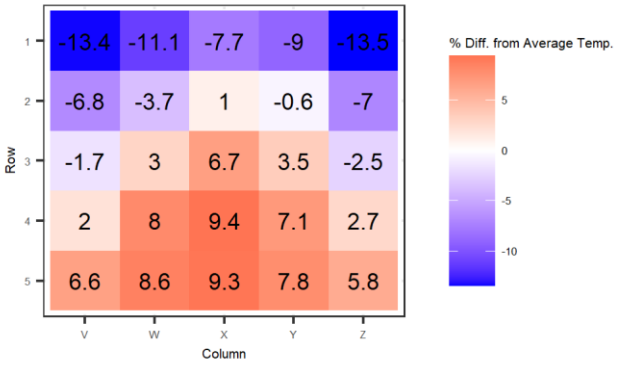


Temperature Stratification, Test ID 031:8:1:160:100%

Avg. Temp. = 89 degF

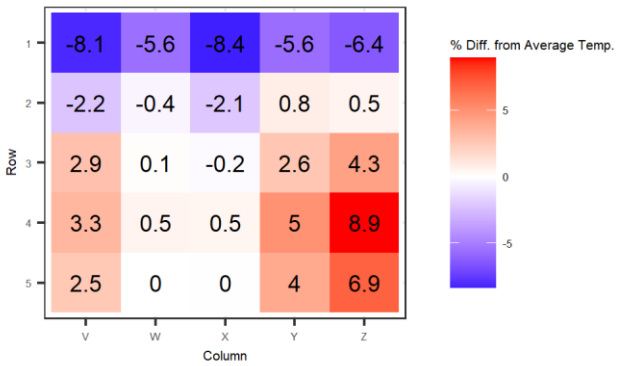


Temperature Stratification, Test ID 027:12:2:120:27%

Avg. Temp. = 87 degF

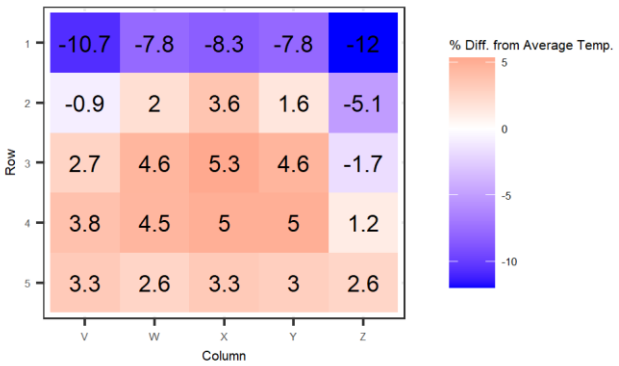


Temperature Stratification, Test ID 026:12:2:120:37%

Avg. Temp. = 89.92 degF

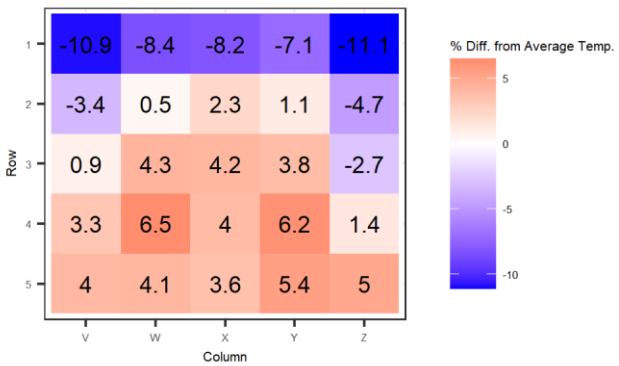


Temperature Stratification, Test ID 025:12:2:120:59%

Avg. Temp. = 90 degF

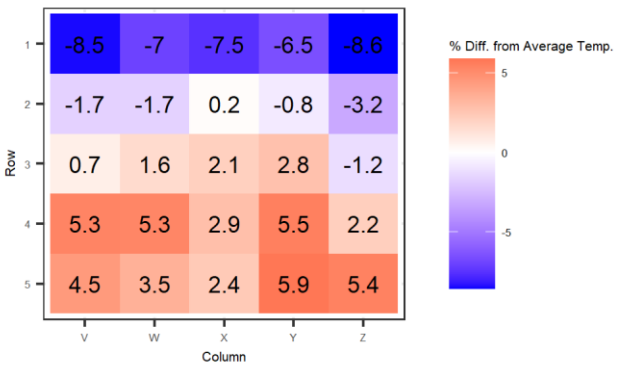


Temperature Stratification, Test ID 024:12:2:120:100%

Avg. Temp. = 90 degF

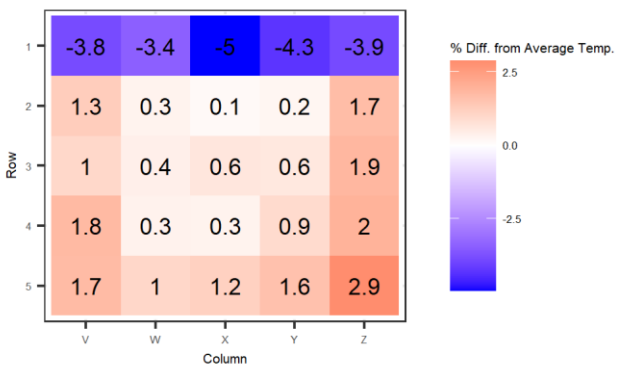


Temperature Stratification, Test ID 023:12:2:160:27%

Avg. Temp. = 91 degF

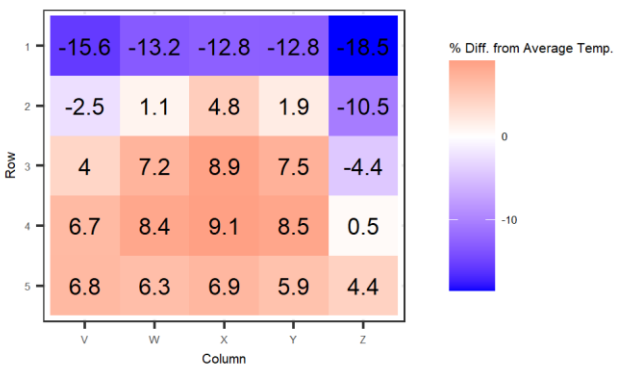

Temperature Stratification, Test ID 022:12:2:160:37%

Avg. Temp. = 93 degF

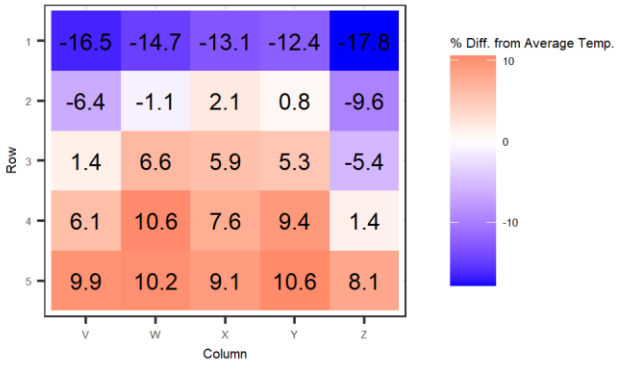


Temperature Stratification, Test ID 021:12:2:160:59%

Avg. Temp. = 93 degF

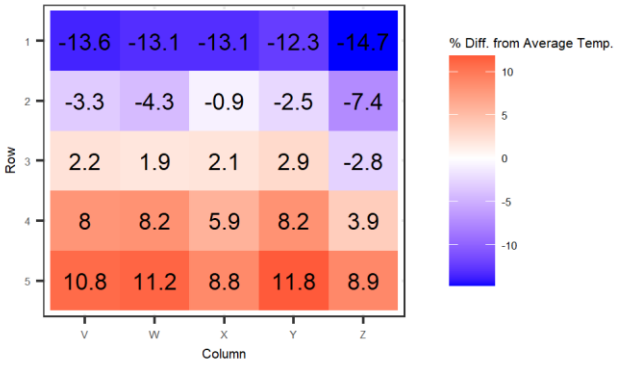


Temperature Stratification, Test ID 020:12:2:160:100%

Avg. Temp. = 92 degF

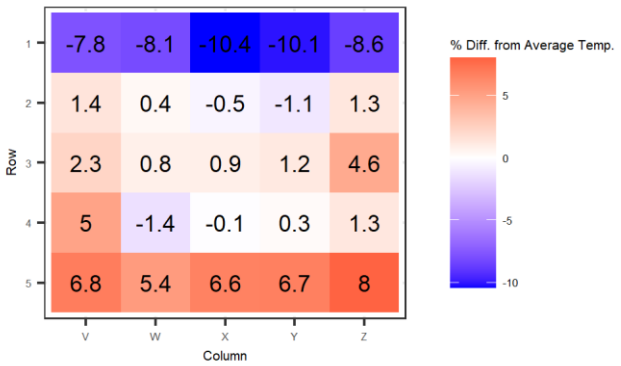


Temperature Stratification, Test ID 019:12:3:120:100%

Avg. Temp. = 86 degF

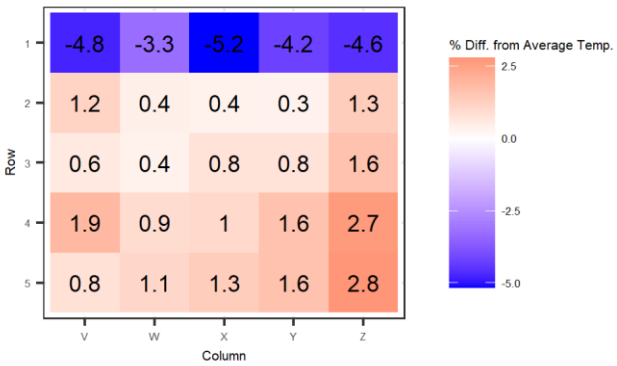


Temperature Stratification, Test ID 018:12:3:120:100%

Avg. Temp. = 89 degF

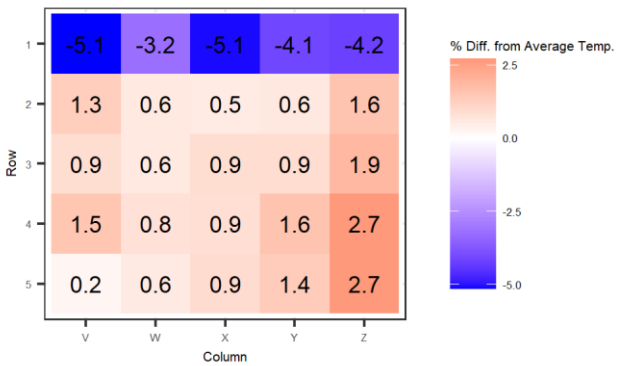


Temperature Stratification, Test ID 017:12:3:120:27%

Avg. Temp. = 88 degF

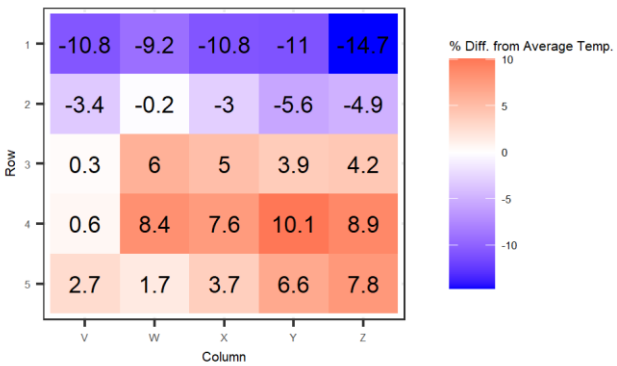


Temperature Stratification, Test ID 016:12:3:120:37%

Avg. Temp. = 89 degF

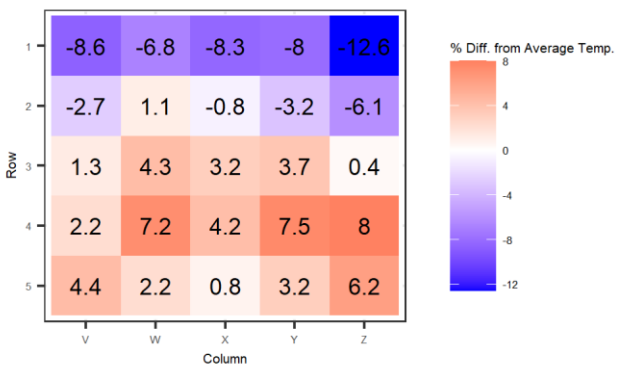


Temperature Stratification, Test ID 015:12:3:120:59%

Avg. Temp. = 89 degF

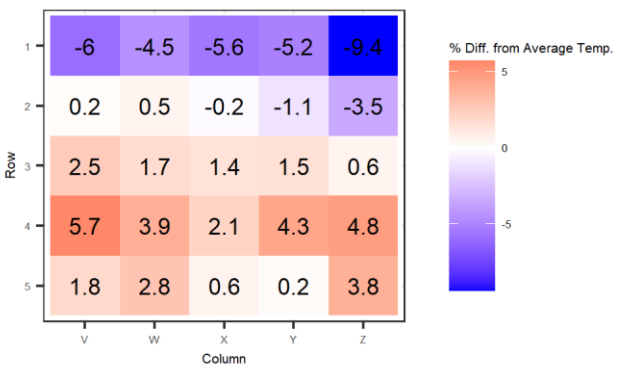

Temperature Stratification, Test ID 014:12:3:120:100%

Avg. Temp. = 89.92 degF

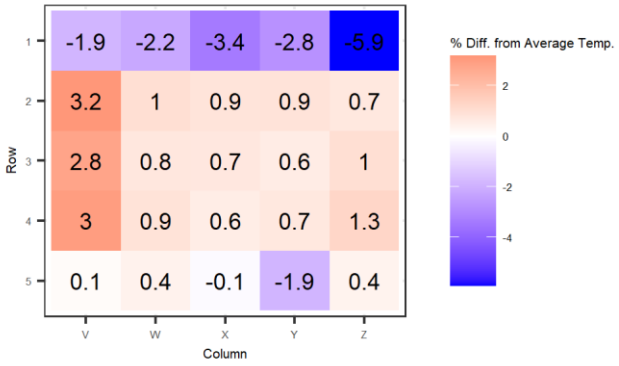


Temperature Stratification, Test ID 004:12:1:160:59%

Avg. Temp. = 89.92 degF

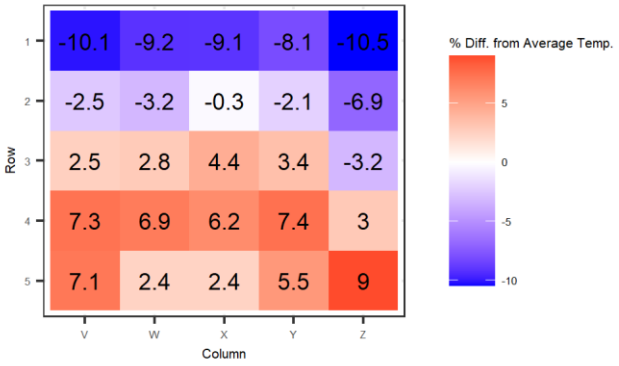


Temperature Stratification, Test ID 003:12:1:160:37%

Avg. Temp. = 87.92 degF

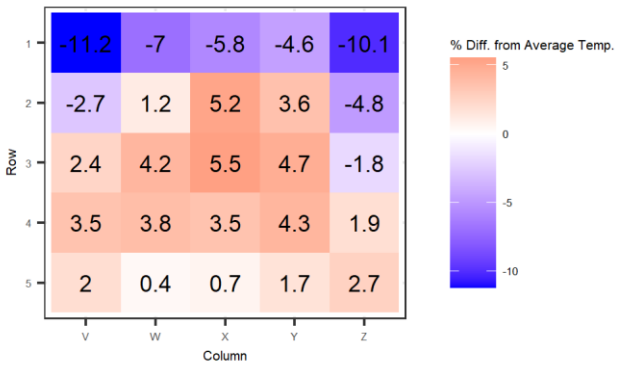


Temperature Stratification, Test ID 002:12:1:160:27%

Avg. Temp. = 84 degF

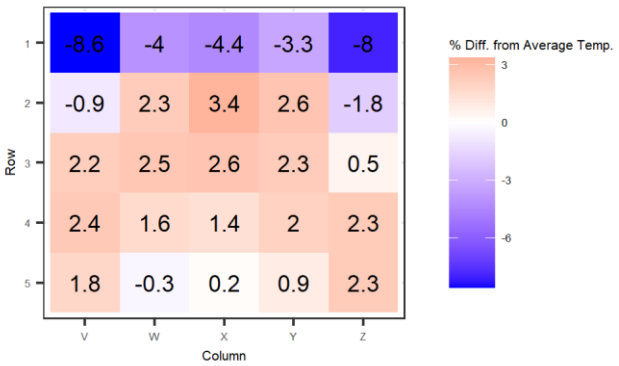


Temperature Stratification, Test ID 001:12:1:160:100%

Avg. Temp. = 88 degF

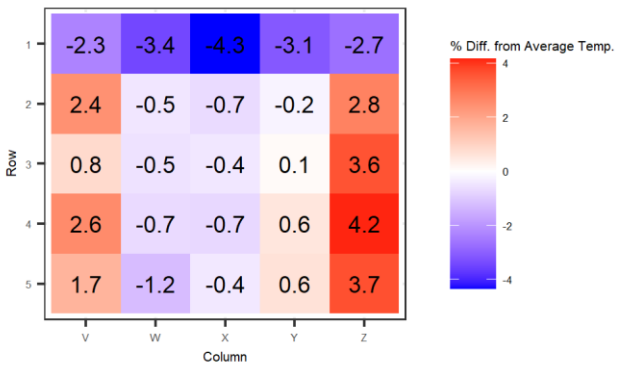

# APPENDIX C:
# Velocity Traverse Measurements Box Plots

Notes:

- Data reflects traverses taken for 35 total tests (data removed for tests in which the damper was flipped as that his atypical).
- A 25-point point traverse was taken for each test, with locations of points selected following the Log-Tchebycheff method in accordance with current NEBB standards.

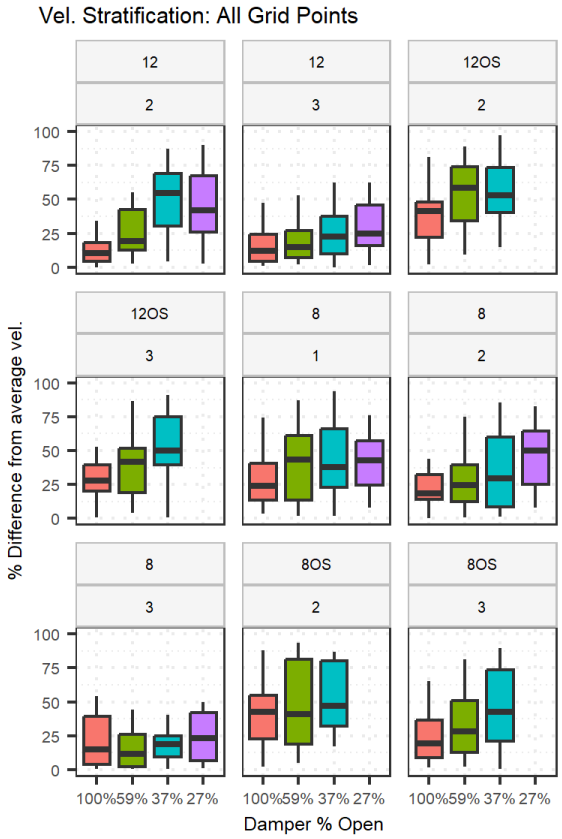


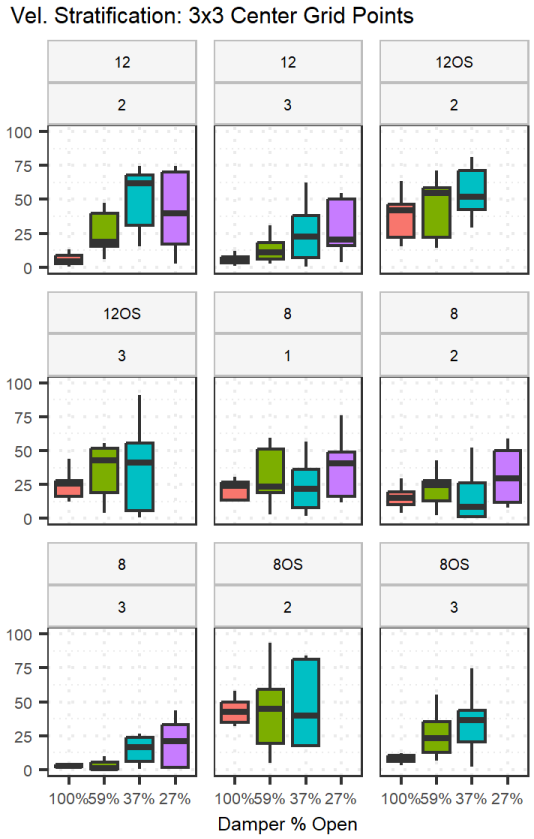

# APPENDIX D:
# Velocity Traverse Measurements Heatmaps

Notes:

- Data reflects traverses taken for 39 total tests (includes tests for which the damper was flipped).
    - Damper was flipped for Test IDs 28:8:1:358:100%, 29:8:1:358:59%, 30:8:1:358:37%, and 31:8:1:358:27%
- Test ID nomenclature is as follows: [traverse order #]:[box size (in.)]:[coil rows]:[CFM]:[damper % open]
    - Test ID **17:8:1:358:59%** therefore indicates the **17th** traverse taken, ran with an **8" box**, a **1-row coil**, at **358 cfm**, with the damper **59% open**.
    - Note that this nomenclature is NOT the same as that used for the heatmaps in Appendix 2.
        - i.e. the 17th traverse taken did not correspond to the 17th test in the experiment.

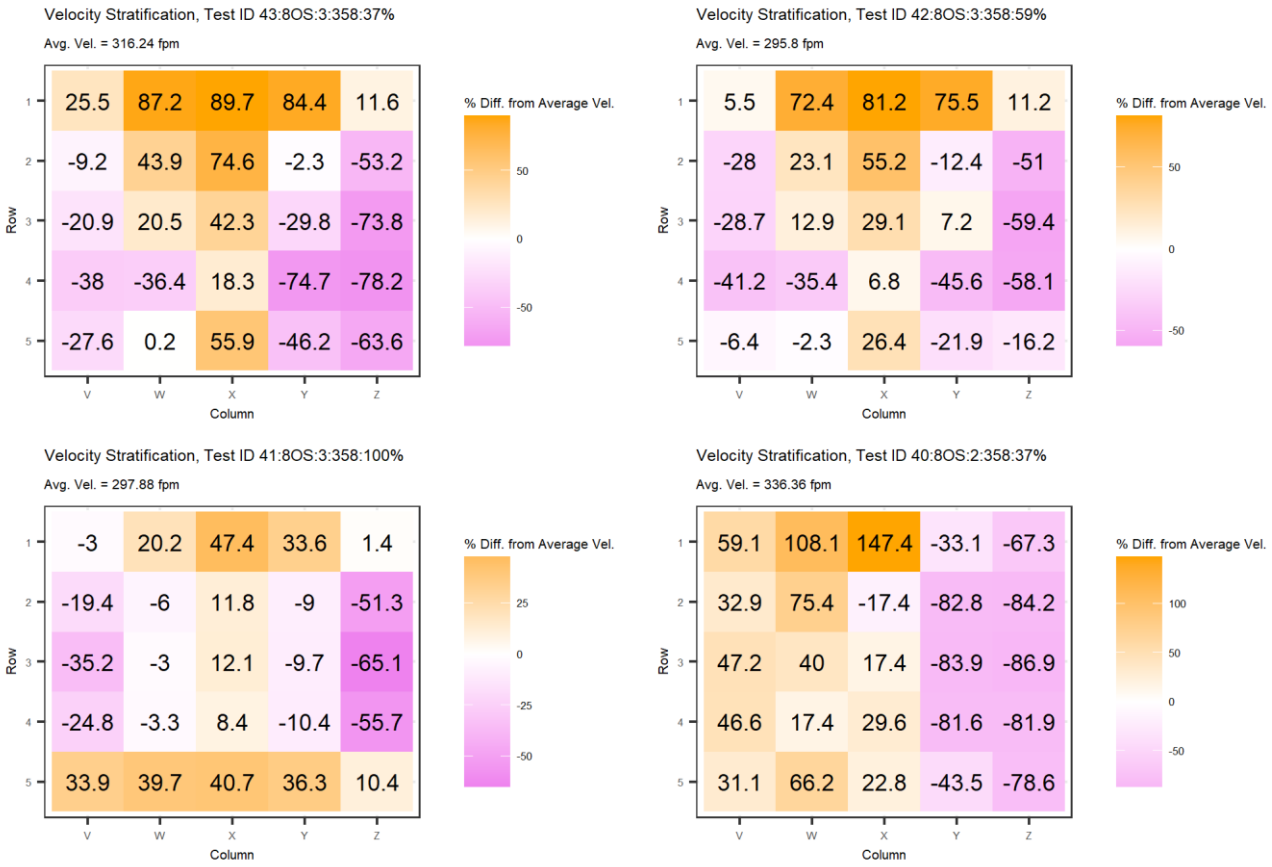

Velocity Stratification, Test ID 39:8OS:2:358:59%

Avg. Vel. = 303.12 fpm

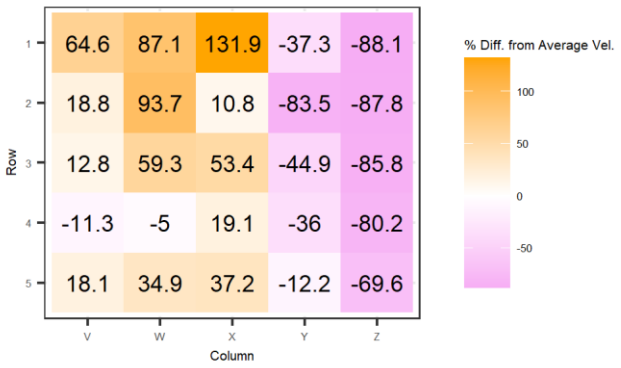


Velocity Stratification, Test ID 38:8OS:2:358:100%

Avg. Vel. = 295.04 fpm

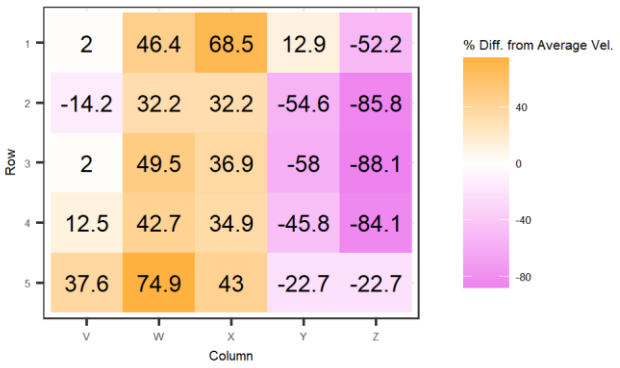


Velocity Stratification, Test ID 37:12OS:3:780:37%

Avg. Vel. = 326.56 fpm

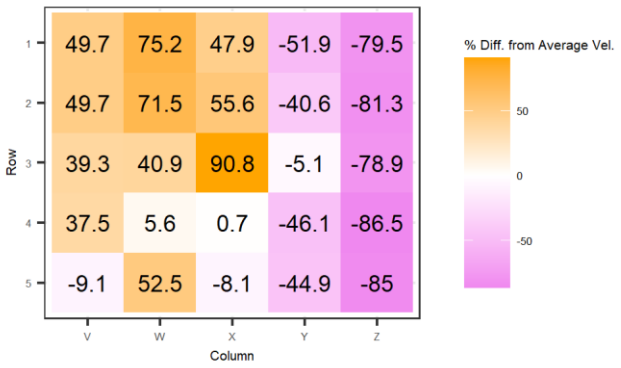


Velocity Stratification, Test ID 36:12OS:3:780:59%

Avg. Vel. = 332.84 fpm

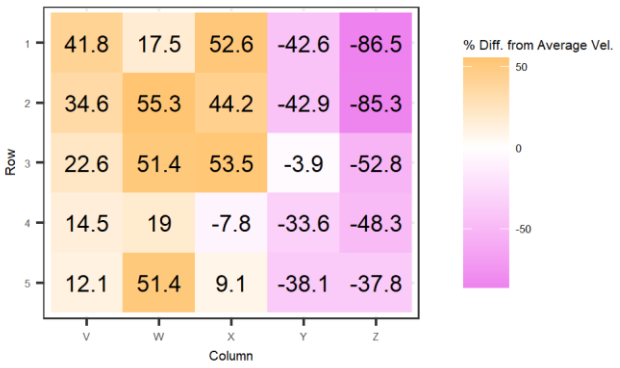


Velocity Stratification, Test ID 35:12OS:3:780:100%

Avg. Vel. = 326.84 fpm

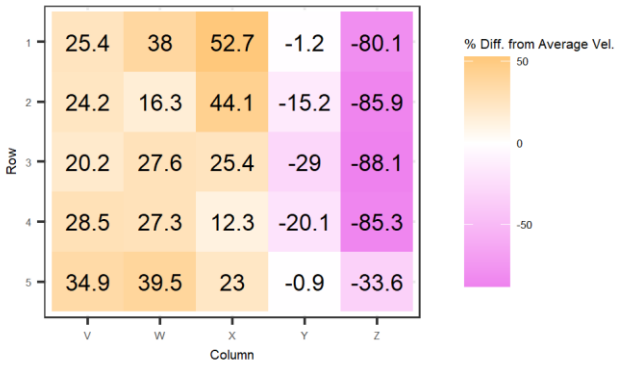


Velocity Stratification, Test ID 34:12OS:2:780:37%

Avg. Vel. = 413.56 fpm

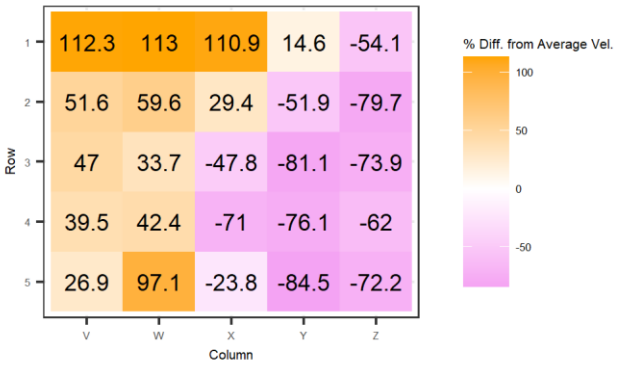


Velocity Stratification, Test ID 33:12OS:2:780:59%

Avg. Vel. = 334.16 fpm

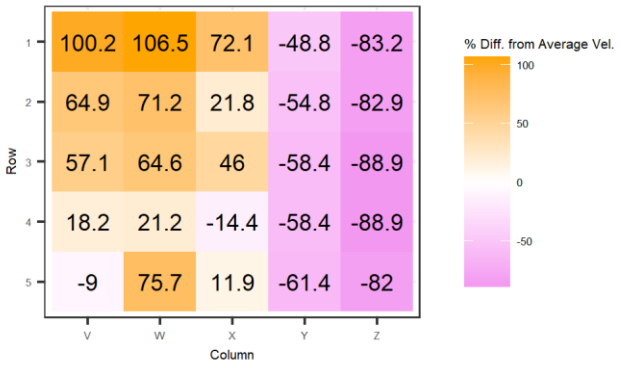


Velocity Stratification, Test ID 32:12OS:2:780:100%

Avg. Vel. = 328.12 fpm

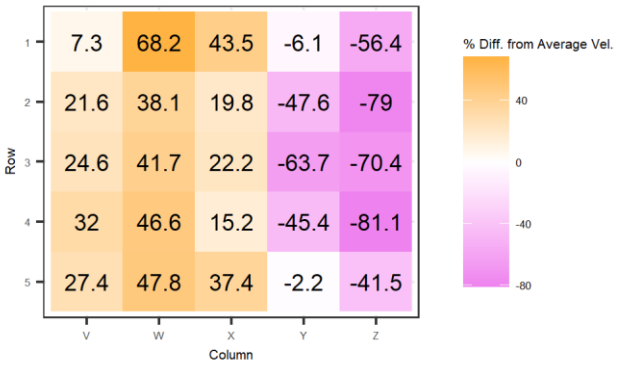

Velocity Stratification, Test ID 31:8:1:358:27%

Avg. Vel. = 653.92 fpm

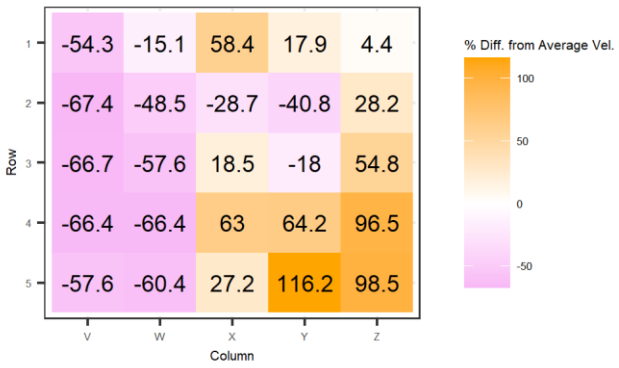


Velocity Stratification, Test ID 30:8:1:358:37%

Avg. Vel. = 561.72 fpm

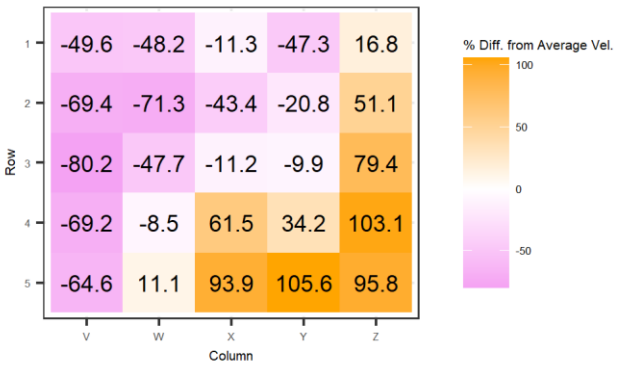


Velocity Stratification, Test ID 29:8:1:358:59%

Avg. Vel. = 476.2 fpm

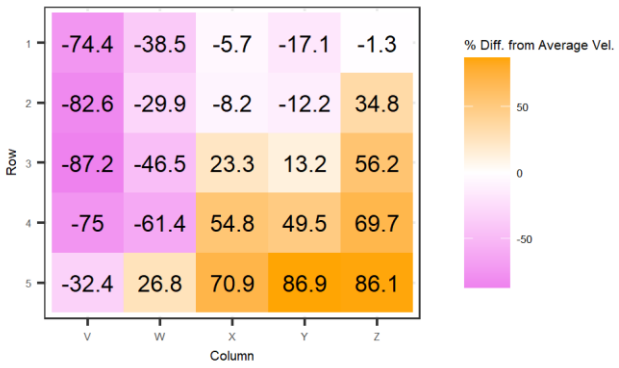


Velocity Stratification, Test ID 28:8:1:358:100%

Avg. Vel. = 449.2 fpm

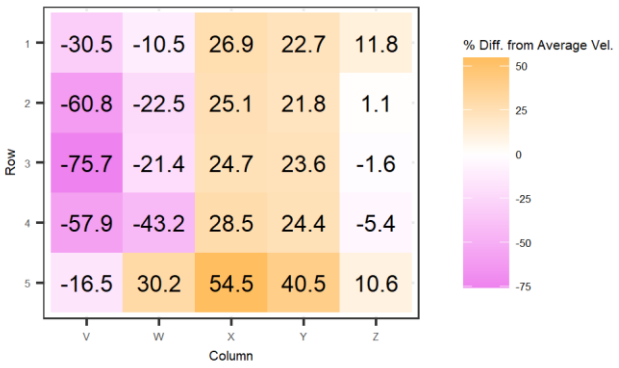


Velocity Stratification, Test ID 27:8:3:358:27%

Avg. Vel. = 437.6 fpm

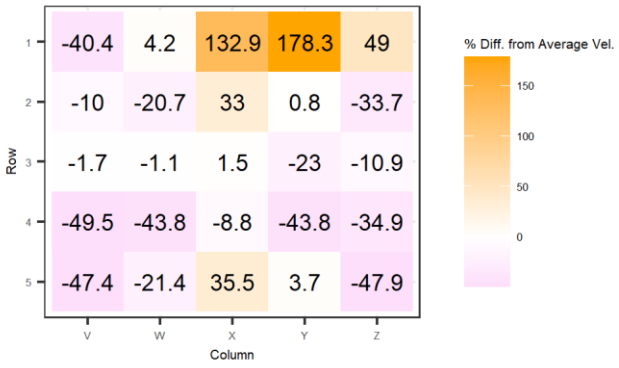


Velocity Stratification, Test ID 26:8:3:358:37%

Avg. Vel. = 412.88 fpm

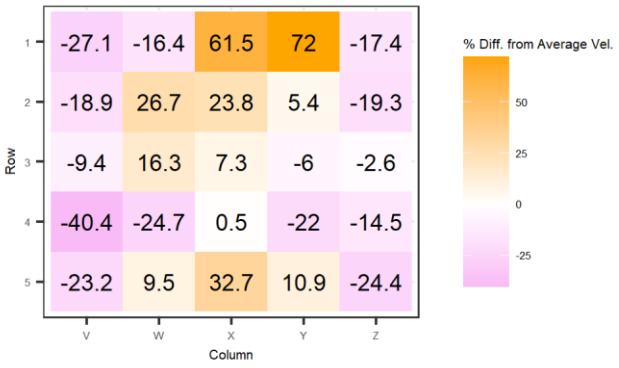


Velocity Stratification, Test ID 25:8:3:358:59%

Avg. Vel. = 415.72 fpm

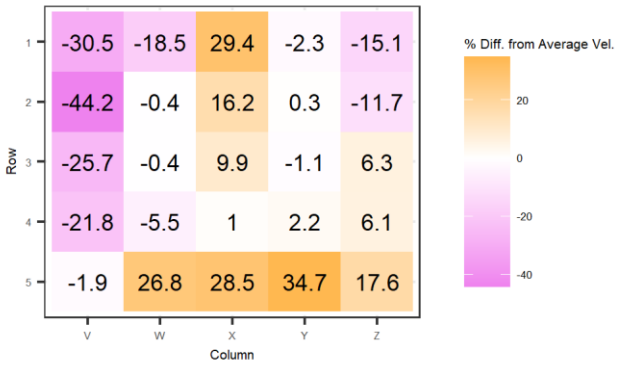


Velocity Stratification, Test ID 24:8:3:358:100%

Avg. Vel. = 437.68 fpm

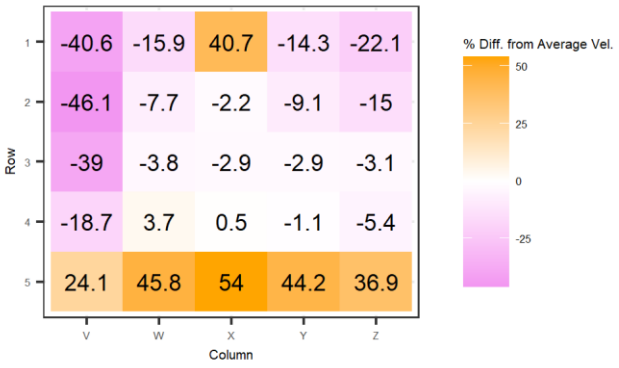

Velocity Stratification, Test ID 23:8:2:358:27%

Avg. Vel. = 393 fpm

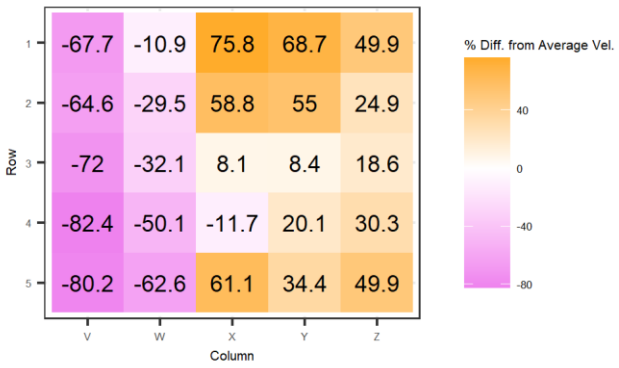


Velocity Stratification, Test ID 22:8:2:358:37%

Avg. Vel. = 408.96 fpm

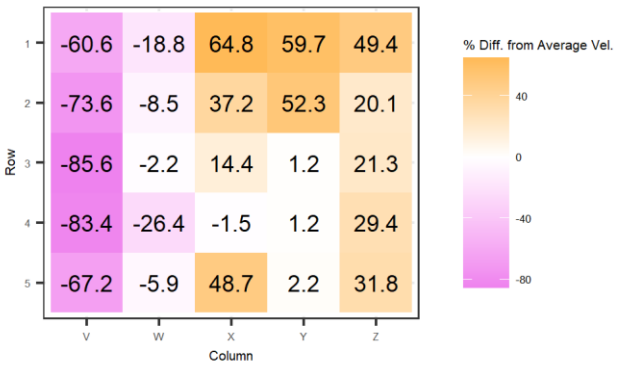


Velocity Stratification, Test ID 21:8:2:358:59%

Avg. Vel. = 423 fpm

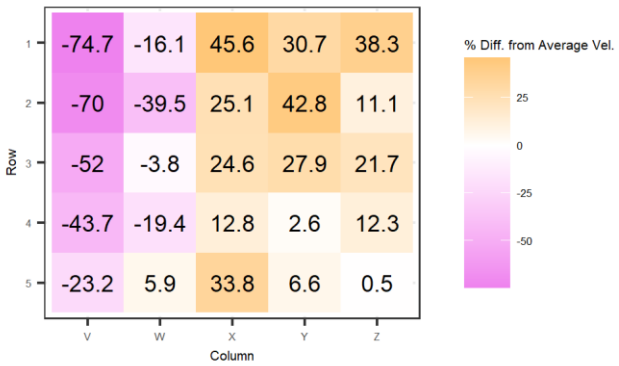


Velocity Stratification, Test ID 20:8:2:358:100%

Avg. Vel. = 431.12 fpm

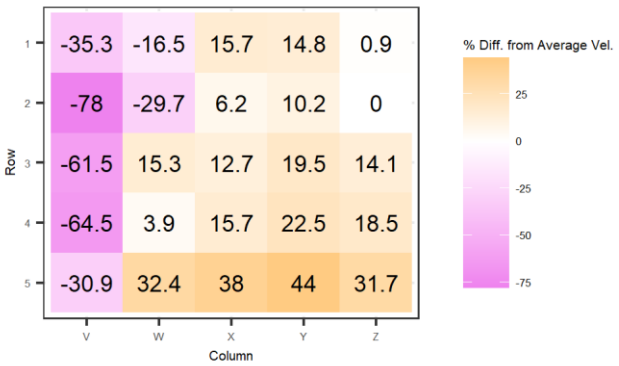


Velocity Stratification, Test ID 19:8:1:358:27%

Avg. Vel. = 478.84 fpm

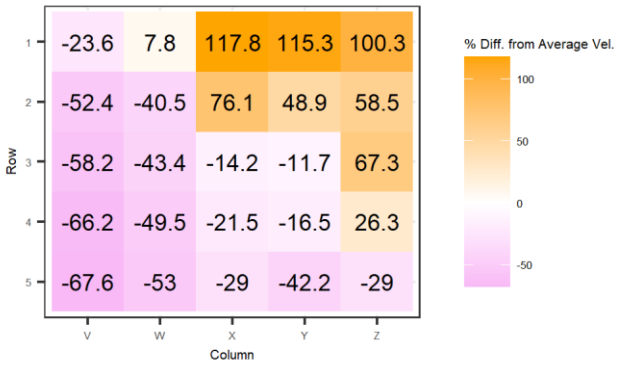


Velocity Stratification, Test ID 18:8:1:358:37%

Avg. Vel. = 463.92 fpm

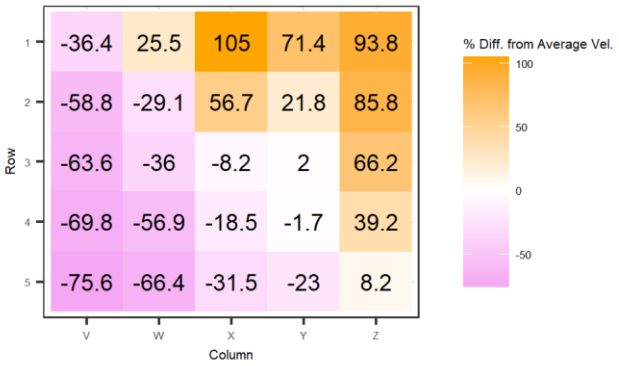


Velocity Stratification, Test ID 17:8:1:358:59%

Avg. Vel. = 440.72 fpm

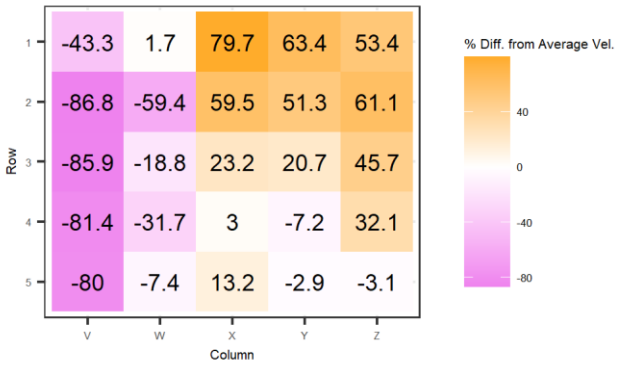


Velocity Stratification, Test ID 16:8:1:358:100%

Avg. Vel. = 455.2 fpm

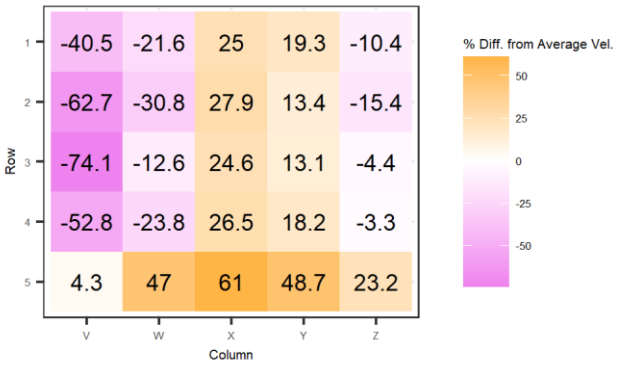

Velocity Stratification, Test ID 15:12:3:780:37%

Avg. Vel. = 466.32 fpm

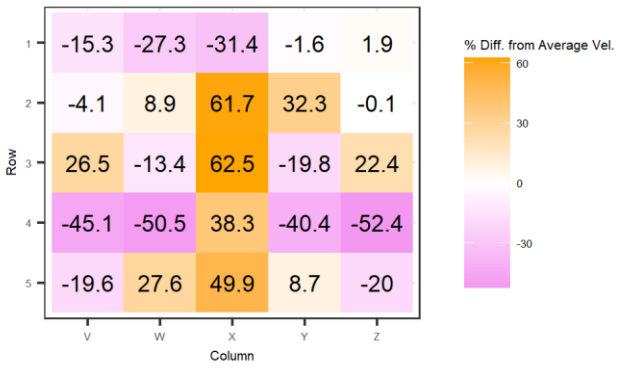


Velocity Stratification, Test ID 14:12:3:780:59%

Avg. Vel. = 460.8 fpm

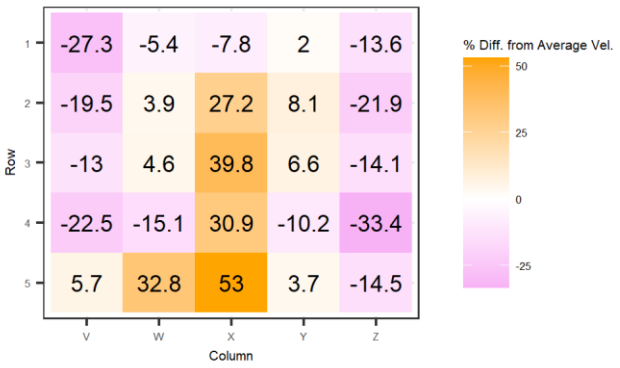


Velocity Stratification, Test ID 13:12:3:780:100%

Avg. Vel. = 447.84 fpm

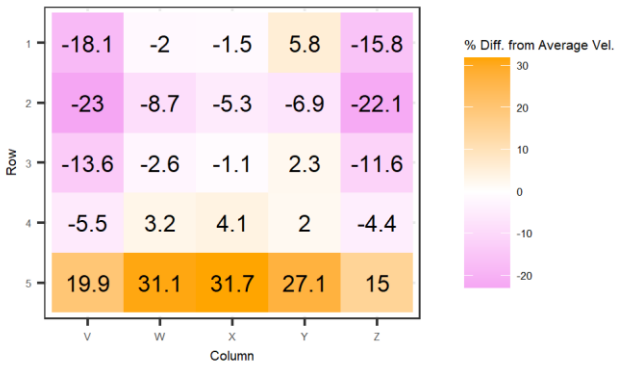


Velocity Stratification, Test ID 12:12:3:780:27%

Avg. Vel. = 374.6 fpm

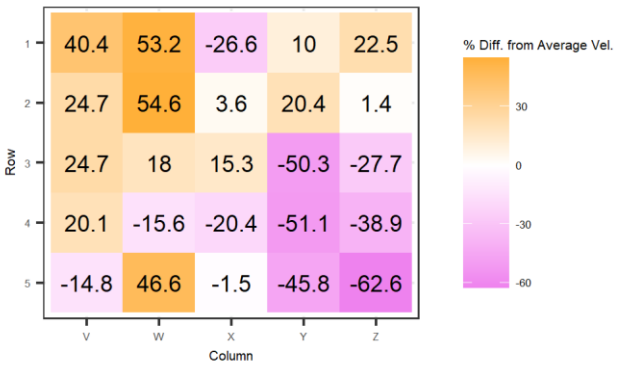


Velocity Stratification, Test ID 11:12:3:780:37%

Avg. Vel. = 398.36 fpm

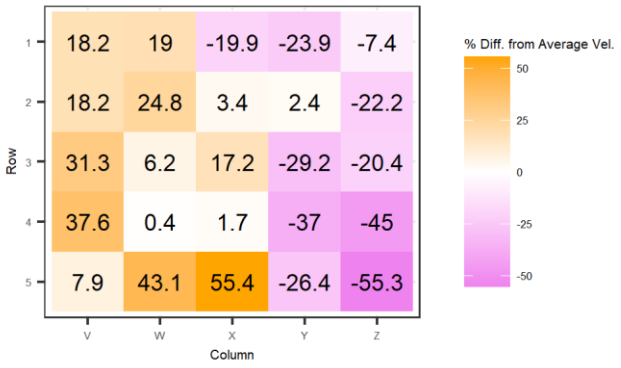


Velocity Stratification, Test ID 10:12:3:780:59%

Avg. Vel. = 395.2 fpm

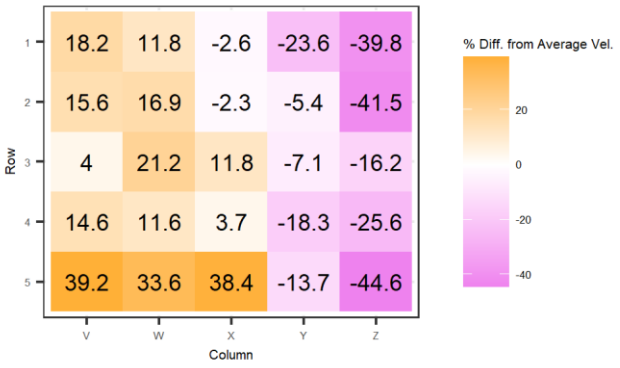


Velocity Stratification, Test ID 09:12:3:780:100%

Avg. Vel. = 401.6 fpm

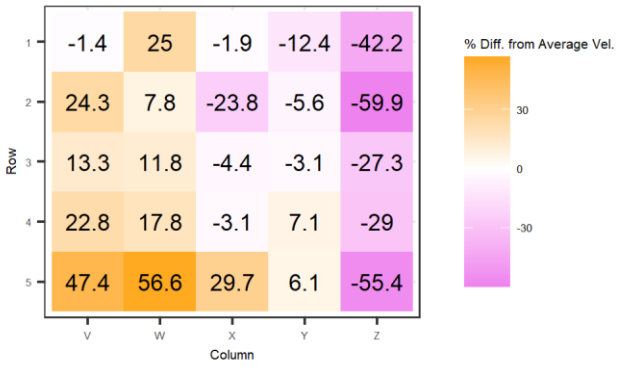


Velocity Stratification, Test ID 08:12:2:780:27%

Avg. Vel. = 546.88 fpm

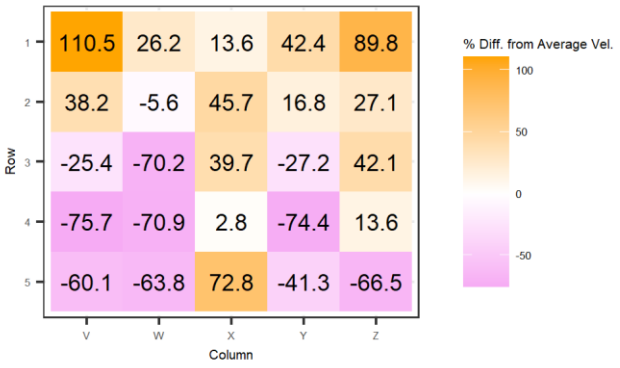

Velocity Stratification, Test ID 07:12:2:780:37%

Avg. Vel. = 476.6 fpm

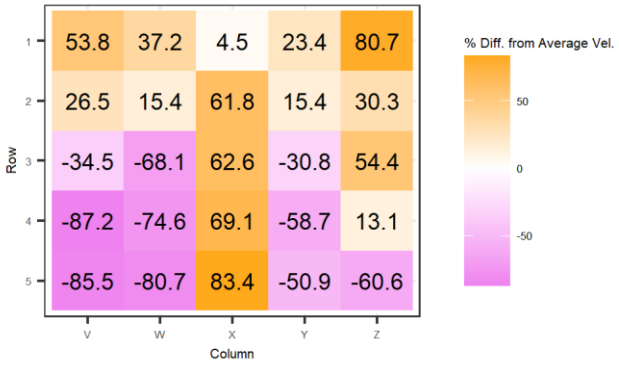


Velocity Stratification, Test ID 06:12:2:780:59%

Avg. Vel. = 428.32 fpm

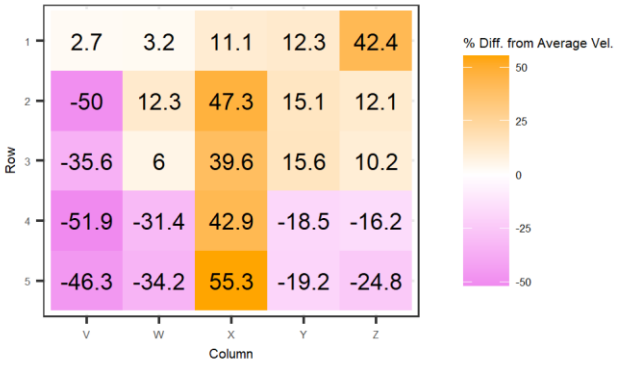


Velocity Stratification, Test ID 05:12:2:780:100%

Avg. Vel. = 423.56 fpm